Journal of proteome research

Open Access

pubs.acs.org/jpr

Article

Differential Proteome Profiling Analysis under Pesticide Stress by the Use of a Nano-UHPLC-MS/MS Untargeted Proteomic-Based Approach on a 3D-Developed Neurospheroid Model: Identification of Protein Interactions, Prognostic Biomarkers, and Potential Therapeutic Targets in Human IDH Mutant High-Grade Gliomas

Kaouthar Louati,* Amina Maalej, Fatma Kolsi, Rim Kallel, Yassine Gdoura, Mahdi Borni, Leila Sellami Hakim, Rania Zribi, Sirine Choura, Sami Sayadi, Mohamed Chamkha, Basma Mnif, Zouheir Khemakhem, Tahya Sellami Boudawara, Mohamed Zaher Boudawara, and Fathi Safta

Cite This: *J. Proteome Res.* 2023, 22, 3534−3558

Read Online

ACCESS | Metrics & More | Article Recommendations | Supporting Information

ABSTRACT: High-grade gliomas represent the most common group of infiltrative primary brain tumors in adults associated with high invasiveness, agressivity, and resistance to therapy, which highlights the need to develop potent drugs with novel mechanisms of action. The aim of this study is to reveal changes in proteome profiles under stressful conditions to identify prognostic biomarkers and altered apoptogenic pathways involved in the anticancer action of human isocitrate dehydrogenase (IDH) mutant high-grade gliomas. Our protocol consists first of a 3D *in vitro* developing neurospheroid model and then treatment by a pesticide mixture at relevant concentrations. Furthermore, we adopted an untargeted proteomic-based approach with high-resolution mass spectrometry for a comparative analysis of the differentially expressed proteins between treated and nontreated spheroids. Our analysis revealed that the majority of altered proteins were key members in glioma pathogenesis, implicated in the cellular metabolism, biological regulation, binding, and catalytic and structural activity and linked to many cascading regulatory pathways. Our finding revealed that grade-IV astrocytomas promote the downstream of the mitogen-activated-protein-kinases/extracellular-signal-regulated kinase (MAPK1/ERK2) pathway involving massive calcium influx. The gonadotrophin-releasing-hormone signaling enhances MAKP activity and may serve as a negative feedback compensating regulator. Thus, our study can pave the way for effective new therapeutic and diagnostic strategies to improve the overall survival.

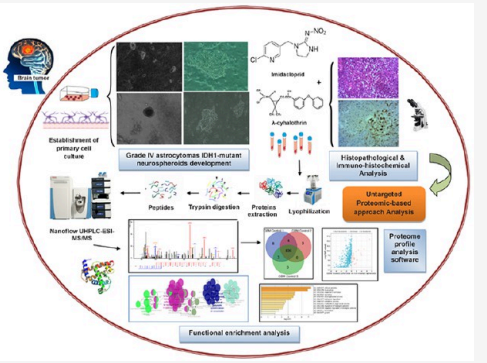

KEYWORDS: *nanoflow UHPLC, tandem mass spectrometry (MS/MS), proteomics, grade-IV astrocytomas IDH mutant, 3D neurospheroids, PPI networks, apoptogenic pathways, neurotoxicity, bioinformatic analysis, gene ontology*

INTRODUCTION

Gliomas are the most common brain astrocytomas constituting about 40% of all primary intracranial tumors. They exhibit various genetic alterations along with phenotypic diversity, contributing to numerous dysregulated pathways. Glioblastoma multiforme, previously categorized under grade-IV gliomas, is the most aggressive, infiltrative, and highly vascularized malignant astrocytoma with a very poor prognosis that cannot be completely eliminated by surgery.[1,2] It occurs mainly in adults with very low survival rates after diagnosis (6 months to 2 years) even if an aggressive treatment involving a combination of surgery, radiotherapy, and chemotherapy is given.[3,4] Moreover, these aggressive tumors express local metastases, with relapse and resistance against a wide range of chemotherapeutic agents.[5,6]

Based on the fifth edition of The World Health Organization (WHO) new classification (2021) of brain tumors and the isolation of isocitrate dehydrogenase (IDH) mutant forms, glioblastomas (GBMs) are now considered biologically and molecularly distinct entities, namely, glioblastoma IDH wild type (IDH-wt), which accounts for more than 90% of all gliomas with a poor prognosis, and grade-IV astrocytomas IDH mutant (IDH-mut).[7]

Received: July 3, 2023
Published: August 31, 2023

Although IDH-mutated gliomas generally exhibit a better disease outcome with prolonged median survival (IDH-wt: 15 months vs IDH-mut: 31 months), tumor recurrence is inevitable over time despite gross total resection and adjuvant chemo-radiotherapy.[8,9] Thus, treatment of the high-grade form is still challenging compared to other solid tumors despite the great advances in medical development and improvements in therapeutic tools such as antiangiogenic reagents, phosphoinositide-3-kinase (PI3K)-mammalian target of rapamycin (mTOR), and epidermal growth factor receptor (EGFR) inhibitors.[10,11] Nonetheless, it remains an urgent need to identify novel mechanistic pathways that may help develop more effective anticancer agents.

Apoptotic cell death plays an important role in the mechanism of anticancer action controlled by several gene families. Targeting the apoptogenic signaling pathways especially in tumors is a promising strategy in oncology.[12]

Pesticides display low molecular weight and high liposolubility that can easily be absorbed and cross all biological membranes, including mitochondrial and hematoencephalic barriers. They have been documented to induce toxicity by generation of oxidative stress following the overproduction of reactive oxygen species (ROS).[13] Disruption in the normal redox state of cells can damage all of their constituents, leading to apoptotic or necrotic cell death, membrane lipid peroxidation, metabolic perturbation as changes in the expression of antioxidant and chaperones, deregulation of several signaling pathways, or alteration of tight junctions.[14−20]

Although the effects of individual pesticides on human health have been studied, neurotoxicity of mixtures is still poorly understood, and few investigations into their potential synergistic effects were conducted on human neuronal and glial cellular systems.

In recent years, insecticides like pyrethroids and neonicotinoids constitute the most widely used class of synthetic pesticides since restrictions have been placed on many of the organophosphorus (OP) and methylcarbamate insecticides which display high mammalian toxicity and low effectiveness due to pest resistance.[21−23] Lambda-cyhalothrin (λ-CYH), a new-generation synthetic type II pyrethroid, is a highly lipophilic compound accumulated in tissues and the most popular due to its high efficacy, easy biodegradability, and low toxicity to mammals and birds.[24−27] Imidacloprid (IMD) is a systemic insecticide belonging to the class of neonicotinoids, which acts on the central nervous system of insects. Both λ-CYH and IMD are widely used mixtures in modern agriculture thanks to their safety at lower concentrations.[28] *In vitro* studies have shown their synergic effect to interfere with the synthesis of purine, guanine, and nucleotides, consequently inducing DNA damage, nuclear abnormalities, and apoptogenic signaling pathways.[29−31] Based on these observations, we have focused on these two molecules to avoid high cytotoxicty effects and make use of their synergic effects to understand the mechanism of anticancer action.

Revealing changes in proteome profiles under stressful conditions has emerged as a key tool for therapeutic target discovery. Also, many relevant *in vitro* models for viability and cytotoxicity studies can serve as biological and analytical platforms for testing chemicals and novel treatments. The use of these assays with state-of-the-art proteomics approaches has increased over recent years in cancer-related fundamental science research due to the development of sensitive and specific mass spectrometry (MS). Thus, it is now possible to analyze dynamic proteome changes, identify proteins and differentially expressed gene signatures with exquisite precision, scrutinize in-depth putative prognostic biomarkers for pathological diagnosis, and elucidate molecular mechanisms that assist in the development of individualized therapeutic strategies to prolong patients' survival.[32]

Therefore, the current study was designed for a comparative analysis of proteome profiles under pesticide stress accessing the major enrichment pathways and the relevance of each protein/gene with its meaningful relationships by the use of an untargeted proteomic approach-based-MS-high-throughput technique on a three-dimensional (3D) *in vitro*-developed neurospheroid model. Our aim is to reflect the process of cell regulation involved in tumor invasiveness and persistence as well as the prognostic biomarkers and altered apoptogenic pathways involved in the anticancer action of IDH mutant high-grade gliomas.

MATERIALS AND METHODS

Chemicals and Materials

IMD (N-(6-chloropyridin-3-ylmethyl)-2-nitro-imino-imidazolidine), $C_9H_{10}ClN_5O_2$ (CAS Number 138261-41-3), and λ-CYH, $C_{22}H_{19}C_{l2}NO_3$ (CAS Number 91465-08-6) were selectively purchased as standard solutions of highest purity (≥98%) from Merck KGaA (Germany) and Sigma-Aldrich Chemie GmbH.

Stock solutions of pesticide mixtures were prepared by diluting 150 mg/mL IMD and 50 mg/mL λ-CYH in ultrapure water containing 0.01% dimethyl sulfoxide (DMSO) (D8418, Sigma). Then, freshly serial diluted solutions were prepared prior to cytotoxicity analysis.

Ultrapure water was prepared with a Millipore purification system (Billerica, MA). Dulbecco's phosphate-buffered saline (PBS) (D8537), Dulbecco's modified Eagle's medium-high glucose (DMEM) (D5796), Ham's nutrient mixture F12 (51651C), L-glutamine (G7513), trypsin-EDTA (T4049), fetal bovine serum (FBS) (F2442), 1% nonessential amino acid solution (NEAA) (100X) (M7145), neuronal viability serum-free medium supplement N2 (100X) (17502048, GIBCO) and B27 (SCM013), recombinant human epidermal growth factor (EGF) (SRP3027), recombinant human basic fibroblast growth factor (bFGF) (GF003AF), and 1% (v/v) penicillin/streptomycin (P4333) were supplied from Sigma-Aldrich.

Single-cell ultralow attachment 60 mm Primaria tissue culture plates (353802) and 25 cm^2 culture flasks (430639) were taken from Corning Life Science (NY). Corning Costar TC-Treated 24-well microplates (CLS3526) were purchased from Sigma-Aldrich.

DL-dithiothreitol (DTT) (3483-12-3), iodoacetamide (IAA) (144-48-9), formic acid (FA) (64-18-6), ammonium bicarbonate (1066-33-7), acetonitrile (ACN) (75-05-8) and methanol (67-56-1) were bought from Sigma (St. Louis, MO). Trypsin (V5280) derived from porcine pancreas was from Promega (Madison, WI).

Ethical Consideration

The procedure carried out in this work was in accordance with the Declaration of Helsinki. It was approved under CPP SUD-0443/2022 by our Ethics Committee related to the Habib Bourguiba university hospital where this study was conducted. Dr Khemakhem et al. confirmed that our study was in accordance with the Code of Ethics adopted by the World Medical Association since it is only applied to patients

https://doi.org/10.1021/acs.jproteome.3c00395
J. Proteome Res. 2023, 22, 3534−3558

(vulnerable groups) and cannot be carried out in a non-vulnerable group. A written informed consent was obtained from each patient before undergoing any neurosurgery for a possible risk of paralysis or mortality. Additional informed consent was obtained from the selected participants, whose identifying information is included in this article.

Sample Collection and Neurospheroid Culture

Six specimens of human brain tumors were collected; then, in parallel experiments, six derived neurospheroids in the cultivation medium were developed for proteomic analysis (three treated spheroids vs three controls). We had tested two protocols based on enzymatic and nonenzymatic dissociation methods described in the Supplementary File, with the aim to develop the most vigorous morphological shape of neurospheroids.

To further determine the ability of spheres' self-renewal to form secondary spheres or subspheres, neurospheroids were gently dissociated into single cells, plated in single-cell ultralow attachment plates, and maintained in a neural stem cell-culture medium.

We visually inspected spheroid health and growth under an inverted phase contrast bright-field microscope (MOTIC AE21, Motic Incorporation Ltd. Hong Kong, China), equipped with an AXIOCAM CAMERA 208 (Sony CMOS image sensor color, Rolling Shutter; square pixels of 1.85 μM side length; 3840 × 2160 pixel resolution; Ultra-HD (4K); 3 × 8-bits/pixel) (Zeiss, France) at scale bars of 100 and 150 μm before proceeding. Images were imported and analyzed by the Image-Pro Plus analyzer software, V7.0 (Media Cybernetics, Inc., Bethesda, MD) (www.adept.net.au/software/mediacy/ImagePro/imageProPlus.shtml, RRID: SCR_007369).

Immunohistochemical (IHC) Staining

Primary cell identity was confirmed prior to use by IHC for neuronal cell markers. "Stemness" gene expressions were also analyzed including CD133 (BD Biosciences Cat# 747569, RRID: AB_2744141), CD44 (BD Biosciences cat. no. 558739, RRID: AB_397098), Nestin (IMGENEX Cat. No. IMG-6492A, RRID: AB_2033866), Vimentin (VIM) (Abcam catalog no. 4211-1, RRID: AB_765097), SOX2 (BD Biosciences catalog no. 560291, RRID: AB_1645334), βIII-tubulin (Promega catalog no. G7121, RRID: AB_430874), GFAP (Aeonian Biotech Cat# AE00178, RRID: AB_2750965), and IDH1 (Proteintech catalog no. 12332-1-AP, RRID: AB_2123159).

Both primary cells and multiple 3D spheroids were harvested and processed into histological blocks that after standard fixation and embedding procedures were sectioned to produce slides for IHC staining.

Chemical Treatment

We have adapoted the protocol described by Roper & Coyle at the University of Nottingham studying the cytotoxicity effect of drugs on a 3D *in vitro*-developed neurospheroid model.[33] Before pesticide treatment was added, the coefficient of variation (CV) in spheroid volumes was measured to confirm growth uniformity (eq A and eq B).

From our preliminary investigations conducted on meningiomas (MNGs) assessing the appropriate cytotoxic inhibitory concentrations (ICs) on human brain tumor neurospheroids, five serial diluted concentrations of pesticide binary mixtures were used ranging from 2.95 μM (754 ng/g) to 0.59 mM (151 × 10^3 ng/g) of IMD and 0.55 μM (247 ng/g) to 0.11 mM (49.5 ng/g) of λ-CYH. We gently removed 100 μL of the neurosphere medium from each plate and added 100 μL of pesticide mixture and then incubated for 24 h in a humidified incubator at 5% CO_2/37 °C. Three replicates per concentration were analyzed. Untreated control cells were also used by changing 100 μL of media with 0.01% DMSO. At the end of the exposure period, toxicity end points were determined in both control and exposed neurospheroids.

Monitoring Spheroid Viability

Following pesticide treatment, cell viability was assessed by two different methods—either by microscopically scrutinizing morphological changes in the size and abundance of spheroids or by histopathological analysis of tumor proliferation as follows: pieces of tumor tissues were collected, frozen at −20 °C, cut on a cryostat rotary manual, which is a microtome cutting frozen tissue (MICROM HM 505N), and then fixed and stained with H&E (hematoxylin and eosin), followed by rinsing consecutively with water, 95% alcohol, and xylene before attachment with a special glue stick for preservation. For each separate experiment, three replicates were carried out.

Sample Preparation and Protein Extraction

After 24 h of pesticide treatment, our samples, consisting of three treated vs nontreated brain tumor spheroids, were harvested, pooled in a centrifuge tube, washed with cold PBS at 4 °C, centrifuged at 2500 rpm for 10 min, and then collected and lyophilized by a freeze-dryer (CHRIST). RIPA Lysis buffer (50 mM Tris−HCl, pH 7.4, 150 mM NaCl, 1% triton X-100, 5 mM EDTA pH 8.0) containing 1× protease inhibitor cocktail (HALT, Thermo scientific) and phosphatase inhibitor cocktail (1 mM NaVO4, 50 nM NaF) (Thermo Scientific) was added to the powdered samples, sonicated, and then centrifuged at 12,000 rpm for 15 min at 4 °C. The supernatant was transferred into a new Eppendorf tube, and the protein concentration was determined using a BCA kit. Then, 100 μg of proteins per sample was transferred into Microcon devices YM-10 (Millipore) and centrifuged at 12,000 rpm for 10 min at 4 °C. Subsequently, 200 μL of 50 mM ammonium bicarbonate was added to the concentrate followed by centrifugation and repeated once. After reduction with 10 mM DTT at 56 °C for 1 h and alkylation with 20 mM IAA at room temperature in the dark for 1 h, the device was centrifuged at 12,000 rpm at 4 °C for 10 min and washed once with 50 mM ammonium bicarbonate. Afterward, 100 μL of 50 mM ammonium bicarbonate and free trypsin digestion was added into the protein solution at a ratio of 1:50 and incubated at 37 °C overnight. Finally, the device was centrifuged at 12,000 rpm for 10 min at 4 °C; then, 100 μL of 50 mM ammonium bicarbonate was added into the device and centrifuged and then repeated once. The extracted peptides were lyophilized to a near dryness and then resuspended in 20 μL of 0.1% formic acid before analysis.

Analysis by Nanoflow UHPLC-ESI-MS/MS

Samples were analyzed on the same day by a high-resolution tandem mass spectrometry consisting of an Ultimate 3000 nano-ultrahigh-performance liquid chromatography (UHPLC) system (ThermoFisher Scientific), an ESI nanospray source, a Q Exactive HF mass spectrometer (ThermoFisher Scientific), and a higher-energy collision-induced dissociation (HCD) fragmentation mode.

The nanocolumn comprised a trapping column (PepMap C18, 100 Å, 100 μm × 2 cm, 5 μm) and an analytical column (PepMap C18, 100 Å, 75 μm × 50 cm, 2 μm). The loaded sample volume was 1 μg, and the total flow rate was 250 nL/min.

https://doi.org/10.1021/acs.jproteome.3c00395
J. Proteome Res. 2023, 22, 3534−3558

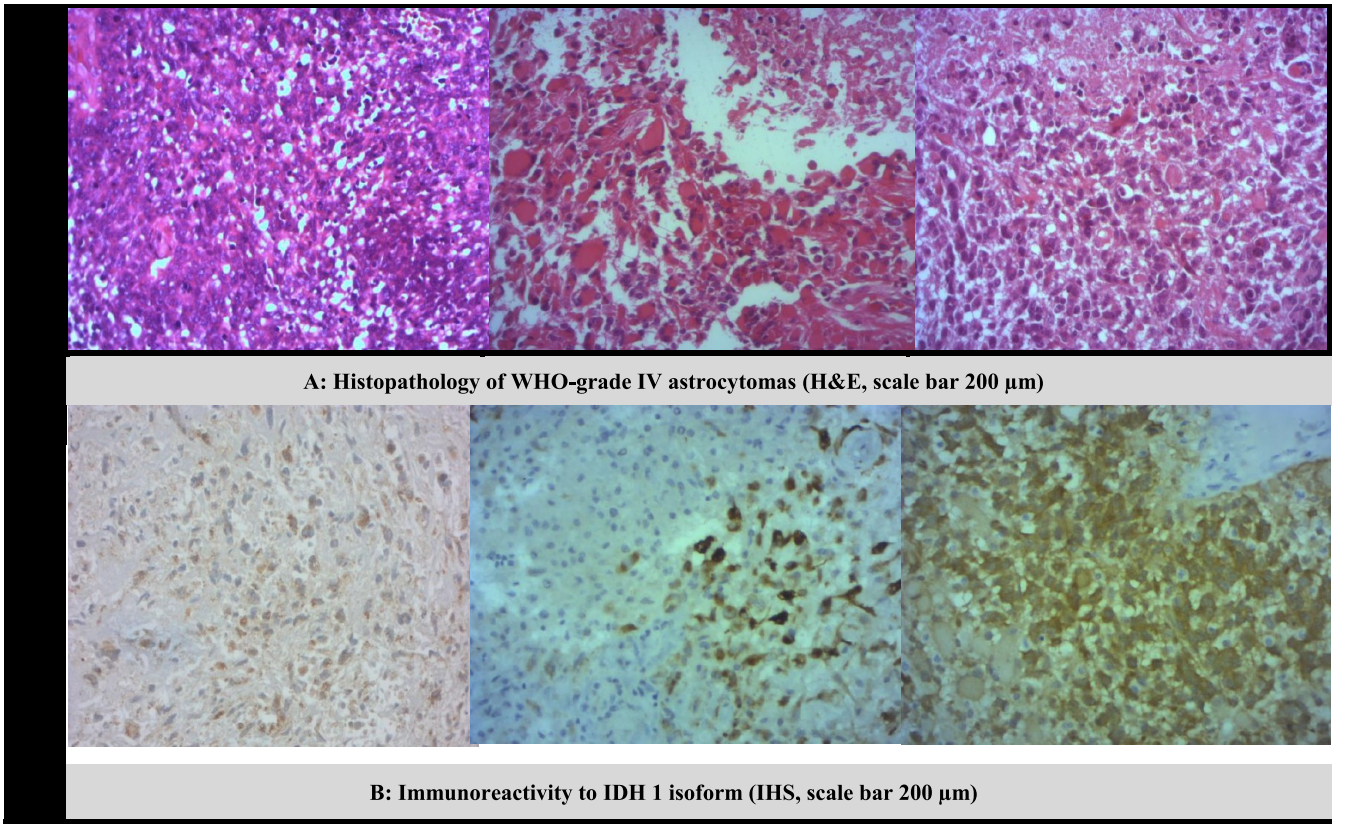

Figure 1. (A) Histopathological diagnosis of high-grade gliomas (WHO grade-IV astrocytomas): high cellularity diffuse proliferation with hyperplastic endothelial cells (H&E × 200). (B) Immunoreactivity of tumor cells with the isoform IDH1, confirming the diagnosis of the IDH mutant WHO grade-IV astrocytomas (IHS × 200). H&E, Hematoxylin & Eosin; IHS, immunohistochemical staining.

The mobile phase comprised solvent A (0.1% formic acid in water) and solvent B (0.1% formic acid in 80% acetonitrile) by linear gradient: from 2 to 8% buffer B in 3 min, from 8 to 20% buffer B in 56 min, from 20 to 40% buffer B in 37 min, and then from 40 to 90% buffer B in 4 min.

The full scan was performed between 300 and 1650m/z at the resolution 60,000 at 200m/z. The automatic gain control target for the full scan was set to 3e6. The MS/MS scan was operated in the Top 20 mode using the following settings: resolution 15,000 at 200m/z; automatic gain control target 1e5; maximum injection time 19 ms; normalized collision energy at 28%; isolation window of 1.4 Th; charge state exclusion: unassigned, 1, ≥ 6; dynamic exclusion 30s.

Data-MS Analysis and Protein Identification

Raw MS files were analyzed and searched against the human protein database based on the species of the samples using MaxQuant (V.1.6.1.14, RRID: SCR_014485). The parameters were set as follows: the protein modifications were carbamidomethylation (C) (fixed) and methionine oxidation (variable); the enzyme specificity was set to trypsin with two maximum missed cleavages; the precursor ion mass tolerance was 10 ppm; and the MS/MS fragment ion tolerance was 0.6 Da.

Proteins were identified with a high confidence interval at 95%, containing at least one identified peptide. The proteome profiles between the two groups were compared using a false discovery rate (FDR) of ≤0.05 as the threshold to judge the significance in protein expression maps' difference. Only proteins identified three times were considered.

Proteins were filtered into two categories, namely, "upregulated" with positive values and "downregulated" with negative values based on the $\log_2$ FC criteria and by a paired t test with a P value threshold of 0.05. Scaffold (version 4.10.0, Proteome software, Inc., Portland, OR) was used to validate the MS/MS-based peptide and protein identification. Heatmaps were plotted by (https://www.bioinformatics.com.cn/en), a free online platform for data analysis and visualization.

Bioinformatic Analysis

We had scrutinized names of proteins/genes by the use of Human Protein Atlas, which is a freely available interactive resource offering the possibility of exploring the proteomes in tissues and organs.[34] Annotations of the identified proteins to their ontology terms were carried out based on their biological process (BP), molecular function (MF), and cellular component (CC). Gene ontology (GO) enrichment analysis was performed by the PANTHER database (version 17.0), which provides comprehensive information about the evolution of protein-coding gene families.[35] For a better understanding of the molecular relationships between each protein/gene function from their various biological processes, a pathway enrichment analysis of regulated proteins at proteomic levels was performed using METASCAPE[36,37] and PANTHER databases. Further, to ensure consistency between the GO and pathway enrichment, a ClueGO (Version 2.5.9) & CluePedia (Version 1.5.9) of the Cytoscape plug-in module (software 3.9.1) analysis integrating both GO terms and pathway annotation was performed to create inter-relational networks.[38−40] In addition, hub genes were predicted by the protein−protein interaction (PPI) network analysis using STRING (Search Tool for the Retrieval of Interacting Genes/Proteins) database version 11.0.[40] The minimum combined score of the hub gene network was set to

https://doi.org/10.1021/acs.jproteome.3c00395
J. Proteome Res. 2023, 22, 3534−3558

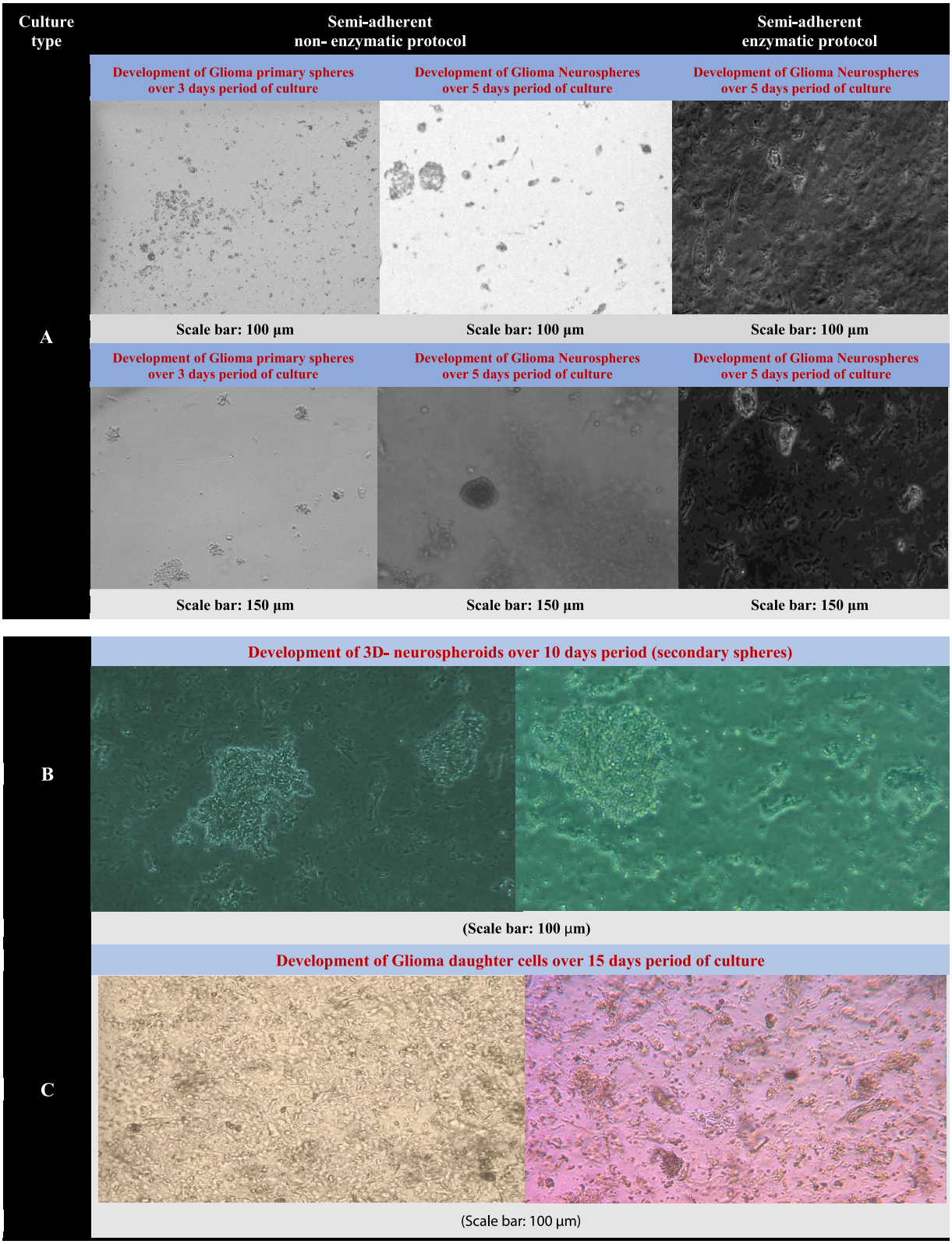

Figure 2. 3D-spheroid culture model of glioma stem-like cells before pesticide treatment. Representative images of 3D-spheroid growth by an inverted phase contrast microscope MOTIC AE21 (Motic Incorporation Ltd. Hong Kong, China), equipped with an AXIOCAM CAMERA 208 (Sony CMOS image sensor color, Rolling Shutter; square pixels of 1.85 μM side length; 3840 × 2160 pixel resolution; ultra-HD (4K); 3 × 8-bits/pixel) (Zeiss, France). Selected images were performed with magnifications of 100 and 150 μm. *By nonenzymatic protocol*: Glioma stem-like cells gave rise to homogeneous cells having a fusiform format and arranged in multidirectional bundles, called primary spheres (A, left panels). After two additional days, primary spheres gave rise to neurospheres (A, middle panels) with self-renewal features such that they continuously formed secondary spheres or subspheres on day 10 (B). *By enzymatic cell dissociation protocol*: Neurospheres derived straight from fresh tumors have a less developed and robust morphology than those isolated from a tumor primary culture (A, right panels). After 15 days, both types of developed 3D neurospheroids could form

https://doi.org/10.1021/acs.jproteome.3c00395
J. Proteome Res. 2023, 22, 3534−3558

Figure 2. continued

astrocytoma daughter adherent cells, which display extensive neurite outgrowth and begin to extend thick bundles of dendrites outward to have spindle-form or polygonal to amorphous shapes (C).

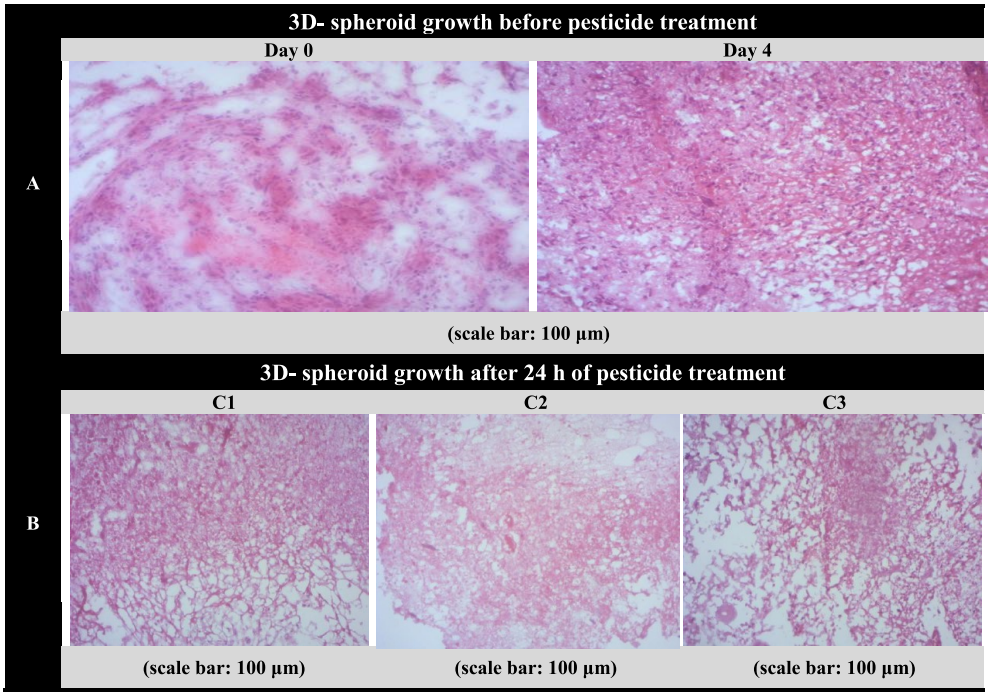

Figure 3. (A) Representative microphotographs of histopathology shown on (H&E) staining obtained from tumor 3D-spheroid sections before and after culture medium. 1: Moderate cell density proliferation on day 0 without culture medium (×100); 2: very high cell density proliferation after 4 days of culture (×100). (B) H&D of 3D-spheroid growth after 24 h of pesticide treatment at three different concentrations (×100). C1: Moderate cell density proliferation; C2: weak cell density proliferation with a light appearance of apoptotic and necrotic cells after a moderate dose of treatment; C3: very weak cell density proliferation with diffuse appearance of apoptotic and necrotic cells after a high dose of treatment.

0.4 by default, but only interactions with a confidence score larger than 0.7 were selected.

RESULTS

Characteristics of Selected Patients

Freshly resected specimens of human brain tumors were collected from patients who underwent surgical procedures in the neurosurgery department of the Habib Bourgiba hospital. Patients' demographics and clinical characteristics are summarized in Supplementary Table S1.

Histological Diagnosis and IHC Staining of Human Brain Tumors

The (H&E) staining shown in Figure 1A identifies the histopathological diagnosis of WHO grade-IV astrocytomas for our collected brain tumor tissues. The IHC staining shown in Figure 1B confirmed isoform IDH1-mutation.

Isolation of Tumor Stem-like Cells, Characterization of Sphere Formation, and Stemness Markers

Glioma stem-like cells (GSCs) gave rise within 3 days of culture to primary spheres arranged in multidirectional bundles with a fusiform format (Figure 2A, left panels). After two additional days, these primary spheres gave rise to neurospheres exhibiting a strenuous morphology with a diameter of 250−350 μm (Figure 2A, middle panels). The CV was inferior to 20%, proving the reproducibility in spheroid size over three different replicates. In the same way, neurospheroids were generated by enzymatic dissociation within 5 days, showing heterogonous morphological shapes (Figure 2A, right panels). Thus, our further experiments were carried out on spheroids isolated from a primary tumor culture to generate a more developed and robust morphology, compared with those isolated straight from fresh tumors.

Both types of neurospheroids showed self-renewal features that they continuously formed secondary spheres or subspheres after 5 additional days (Figure 2B). Then, in-depth analysis of stemness features by IHC staining, spheroid expressed positivity for Nestin, VIM, GFAP βIII-tubulin, and CD44, but lack of CD133+ and SOX2 genes, confirmed later by proteomic analysis.

Assessment of Cell Viability and Proliferation following Pesticide Treatment

From our previous experiments on MNGs, the IC_{50} values (required for 50% growth inhibition) of the pesticide mixture calculated from the dose−response curve by nonlinear regression analysis were, respectively, 30.33 μM (7754.2 ng/g) IMD and 5.75 μM (2584.7 ng/g) λ-CYH. These concentrations were also found suitable to assess the cytotxcity response on GBMs in the range of [IC_{30}−IC_{60}] confirmed by histopathological analysis testing of three different concentrations C1, C2, and C3 of pesticide mixtures at (2.95 μM+0.55 μM), (5.9 μM +1.1 μM), and (0.59 mM+0.11 mM), respectively, of IMD and λ-CYH.

https://doi.org/10.1021/acs.jproteome.3c00395
J. Proteome Res. 2023, 22, 3534−3558

The comparative analysis of microphotographs of neurospheroid stained sections before and after pesticide treatment presented in Figure 3A,B revealed that tumor viability and proliferation decreased progressively by an increase of pesticide concentrations to mitigate cell density with a progressive appearance of apoptotic and necrotic cells.

Bioinformatic Analysis of Differentially Expressed Proteins

From Venn diagrams (illustrated in Supplementary Figure S1), a total of 836 differently expressed proteins were shared between nontreated samples, reduced to 547 by loss in treated samples.

The Volcano plot of the differently expressed proteins, shown in Figure 4, revealed 24 proteins at upregulation (described in Supplementary Table S2), 486 proteins at downregulation, and 37 proteins only yielded in the treated samples (described in Supplementary Table S3).

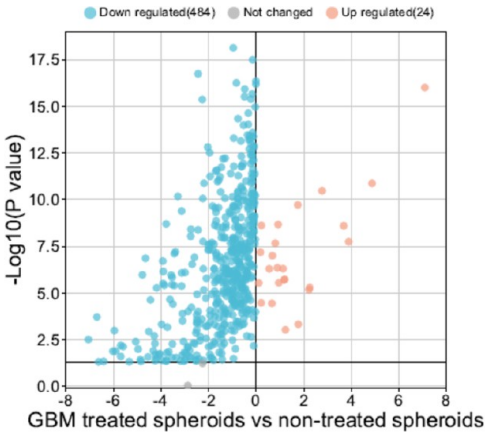

Figure 4. Volcano plot illustrating a total of 510 proteins with increased and decreased expressions following pesticide treatment. The horizontal coordinate is the difference multiple (logarithmic transformation at the base of 2), and the vertical coordinate is the significant difference in *P* value (logarithmic transformation at the base of 10). Data sets were analyzed by setting the cutoff criterion as log2 FC (up: ≥ 0, down: < 0) and a false discovery rate (FDR) ≤ 0.05 as thresholds. The heatmap was plotted by https://www.bioinformatics.com.cn/en, a free online platform for data analysis and visualization.

GO Enrichment Analysis of the Differentially Expressed Proteins. All differentially expressed proteins were mapped to their enriched GO and categorized into three different classes (BP, MF, CC) as illustrated in Figure 5. In terms of MF, the majority of enriched GO terms were involved in binding and catalytic and molecular adaptor activity. As for the BP, genes were found relevant to cellular and metabolic processes as well as biological regulation. For the CC, most proteins were distributed in the cellular part.

Concerning the class of proteins, the majority were related to metabolite interconversion enzymes and cytoskeletal structure (presented in the Supplementary Figure S2).

Pathway Enrichment Analysis of the Differentially Expressed Proteins. The biological significance of the enriched pathways for the annotated genes involved in gliomas was identified. As shown in Figure 6A, the upregulated genes were mainly involved in the apoptotic execution phase, the redox metabolic process, and neural nucleus development. For downregulated genes, the most enriched pathway includes inflammatory mediation, cellular responses to stress, hemostasis, and signaling by Rho GTPases (Figure 6B). For genes only yielded in treated samples, 15 significantly enriched pathways were expressed, as most of them were relevant to the endocrine system, calcium signaling, and WnT and vascular endothelial growth factor (VEGFA, VEGFR2) signaling (Figure 6C).

Furthermore, to ensure consistency between the GO and pathway enrichment, the inter-relational analysis performed using the ClueGO & CluePedia module of Cytoscape with the predicted PPI networks revealed the overexpression of Ca^{2+}-ion export signaling, signal transduction, neuronal development including axon outgrowth, neuronal migration, and chromosome condensation pathways as shown in Figure 7A. The upregulation of the apoptic execution phase, neural nucleus development, redox metabolic process, and thrombin signaling were noticed (Figure 7B). The downregulation was mainly involved in protein folding, signal transduction, and immune-response activities (Figure 7C). The added figures are presented in Supplementary file (Figure S3).

Prediction of Hub Genes through PPI Network Analysis. The PPI network analysis enabled mapping of all of the categories of expressed proteins as well as their degree of connectivity, which helps to reveal their relevance with their meaningful relationships and regulations as well as the identification of hub genes endowed with a pivotal role in the apoptogenic mechanism. In the upregulated class, 32 nodes at diverse strength interactions were revealed, from which 19 prominent hub genes exhibiting connectivity with a high confidence score of 0.7 were identified (presented in Figure 8A).

In the downregulated class, 417 nodes were detected with many hub genes at a high confidence score of 0.9. For proteins only yielded in treated neurospheroids, there were 49 nodes and 28 prominent hub genes at a high confidence score of 0.7 (presented in Figure 8B).

Table 1 lists all of the identified hub genes implicated in the apoptogenic molecular mechanism.

DISCUSSION

Isolation of Neural Stem-like Cells, Characterization of Sphere Formation, and Stemness Markers

Tumor stem-like cells can be defined as tumor-initiating cells[41−50] in which cultured human brain tumor cells could proliferate in a suspension as a 3D conformation not attached to an external surface of the support and generate multipotent floating cell clusters called neurospheres.[51,52]

The 3D growth of established immortalized cell lines or primary cell cultures is regarded as a more rigorous and representative model to perform not only *in vitro* toxicity studies that could best fill the gap left by animal models but also the conventional 2D monolayer cultures that are inherently unable to replicate the 3D environmental complexity and heterogeneity of clinical tumors growing with a specific organization and architecture. In addition, spheroid models provide more biologically congruent data than 2D monolayers due to natural cell-to-cell interactions, hypoxia, drug penetration, response, resistance, and production/deposition of extracellular matrix.[53]

Thus, we have opted for neurospheroid development to address microenvironment remodeling without the confounding effects of exogenous matrices. We have focused on high-grade astrocytomas (grade IV) since the generation of cell cultures from low-grade ones (WHO grades II and III) was reported to be difficult based on only few examples described in the literature.[54] We selected IDH mutation as they are involved in the earliest genetic events in glioma development and in order to make a uniformity analysis avoiding confusing results with

https://doi.org/10.1021/acs.jproteome.3c00395
J. Proteome Res. 2023, 22, 3534−3558

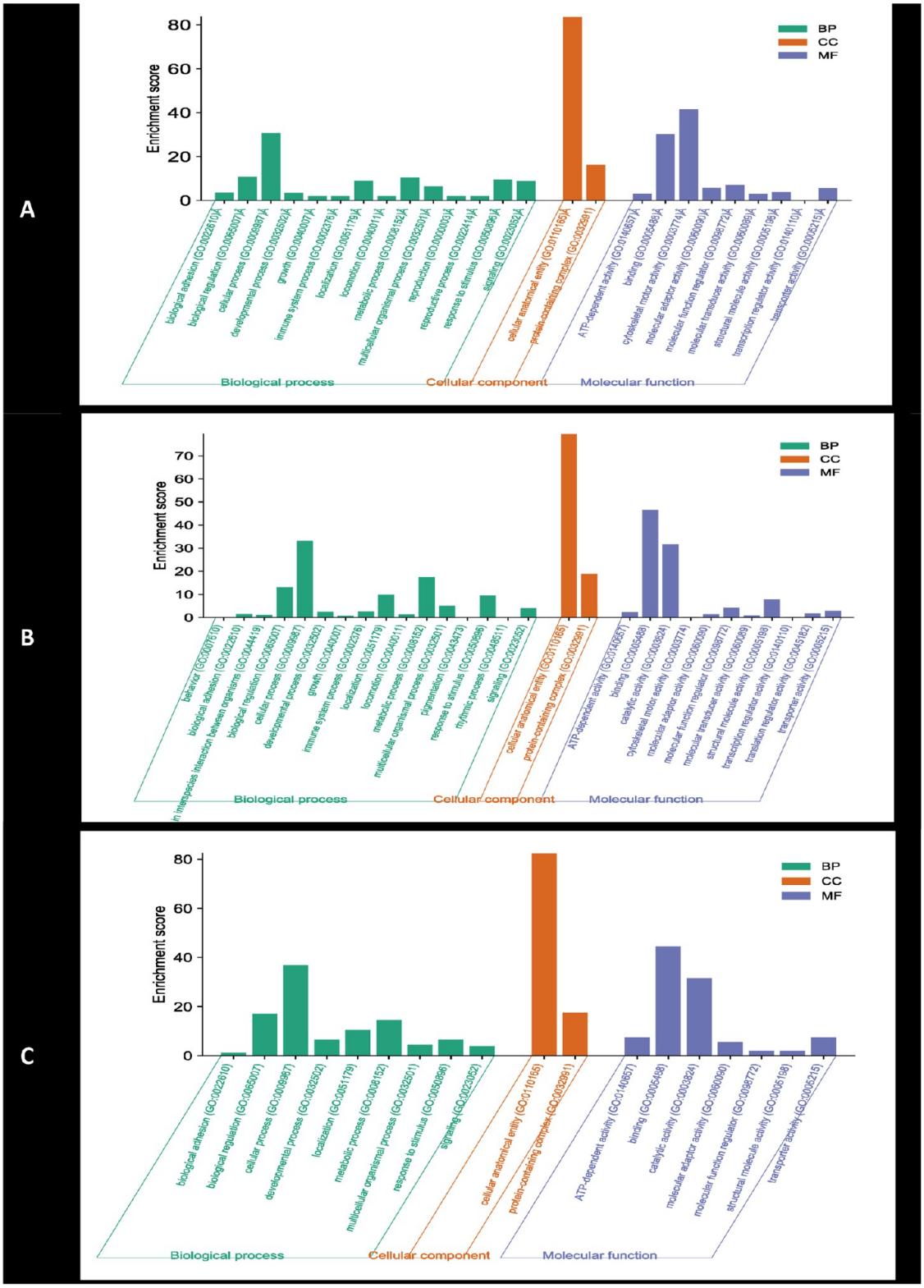

Figure 5. Gene ontology (GO) term enrichment analysis of the differently expressed proteins at upregulation (A), downregulation (B), and only yielded in the treated samples (C) based on three subontologies, namely, biological process (BP), molecular function (MF), and cellular component (CC). The heatmap was plotted by https://www.bioinformatics.com.cn/en, a free online platform for data analysis and visualization.

IDH wild type. IDH1 was the most detected isoform in our case study of gliomas.

Neurospheroids were generated from primary cell cultures to have a more robust morphology than those isolated straight from fresh tumor as confirmed by Pavon et al.[51] After a 5 day culture period, spheres reached a size range of 250−350 μm in diameter, which represents the optimal size that permits drug perfusion and establishes pathophysiological oxygen gradients throughout the spheroid. Contrariwise, spheres with diameters

https://doi.org/10.1021/acs.jproteome.3c00395
J. Proteome Res. 2023, 22, 3534−3558

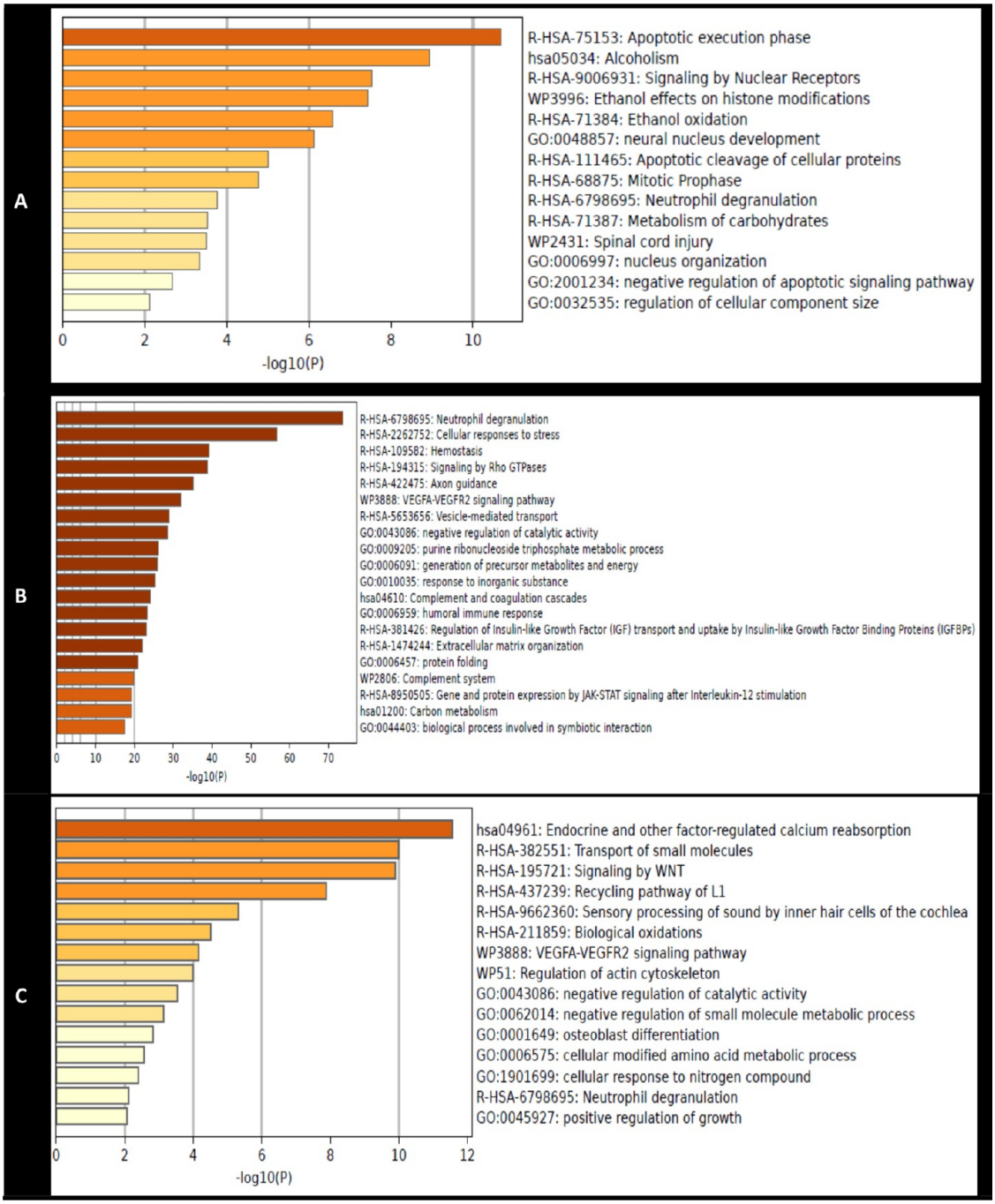

Figure 6. Pathways enrichment analysis with METASCAPE of the differently expressed proteins at upregulation (A), downregulation (B), and only yieded in the treated samples (C).

greater than 500 μm are considered unsuitable as they are characterized by hypoxic regions and necrotic centers.[47]

Before proceeding with cytotoxicity tests, since several morphological parameters, such as spheroid volume and shape, affect the response to treatment with the number of exposed cells that may respond differently to chemicals being a source of variability, and due to the necessity to select tumor spheroids of homogeneous volume and shape in order to reduce data variability to a minimum level, we have proved the reproducibility in spheroid size by calculating the CV of spheroid volumes on day 5 using the Image-Pro Analyzer software described as a perfectly acceptable alternative technique for cytometers.[51] Thus, our 3D spheroids are considered valid models in that they have the same starting dimensions (250−350 μm) and are grown upon the same medium; consequently, drug penetration and media stability will be similar.

Characteristic features of tumor stem-like cells include spherical formation, self-renewal to secondary neurospheres or subspheres, and expression of stem-like markers of their corresponding parental tumors.[55] In our study, we have considered the expression of CD133, CD44, Nestin, VIM, and SOX2 as indicative of stemness markers,[56−59] IDH1 as a diagnostic marker of gliomas,[8] GFAP as an astrocytic marker;[60] and βIII-tubulin as a representative of neuronal differentiated cells.[61] Our developed spheroids have shown enhanced self-

https://doi.org/10.1021/acs.jproteome.3c00395
J. Proteome Res. 2023, 22, 3534−3558

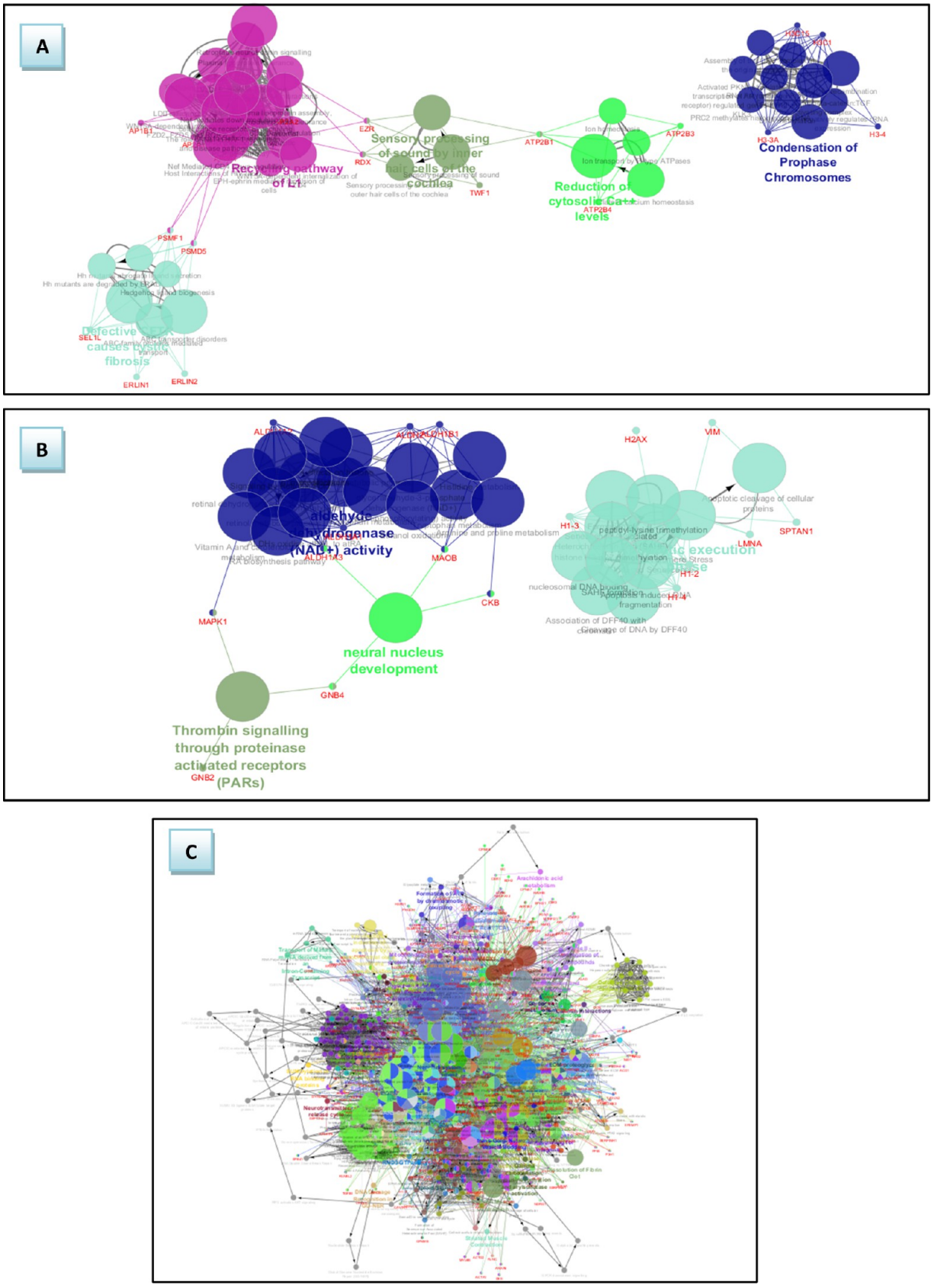

Figure 7. Inter-relational pathway enrichment analysis visualized by the ClueGO & CluePedia Cytoscape plug-in module: (A) for proteins only yielded in the treated neurospheroids; (B) for the upregulated proteins; and (C) for the downregulated proteins.

https://doi.org/10.1021/acs.jproteome.3c00395
J. Proteome Res. 2023, 22, 3534−3558

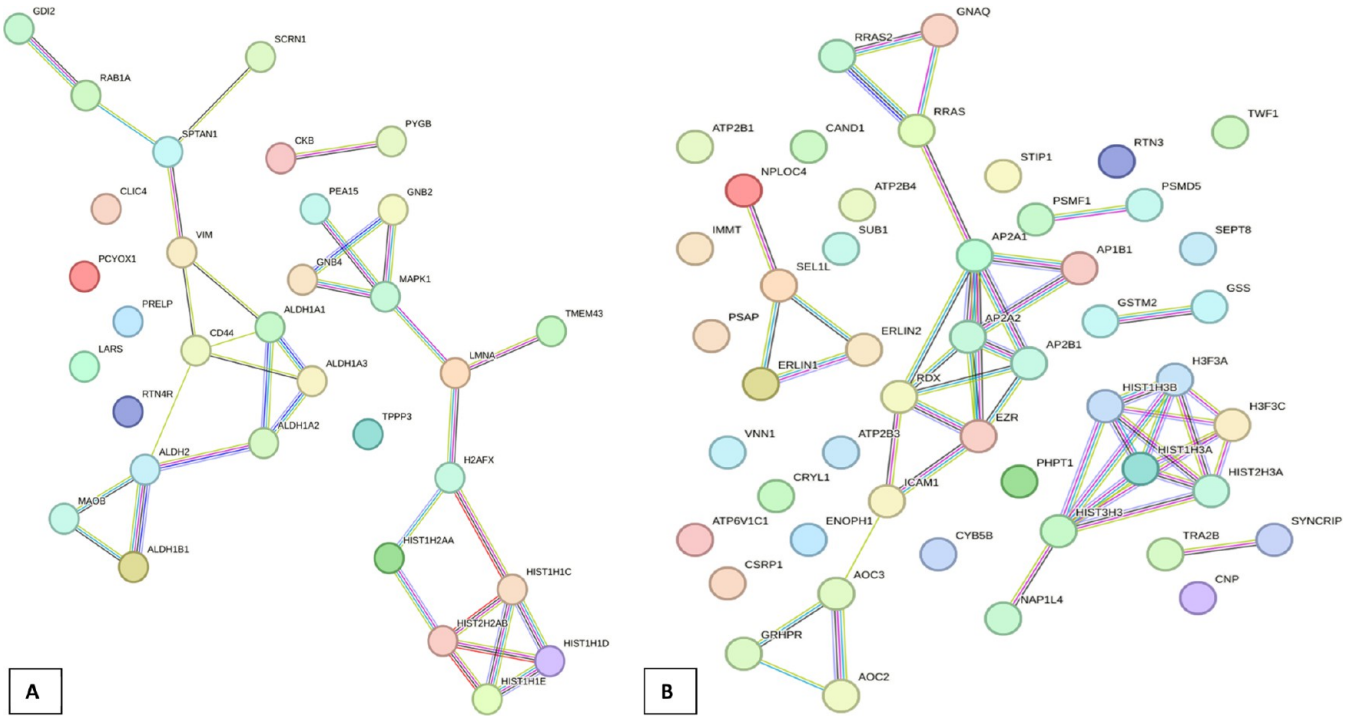

Figure 8. PPI network analysis of the differentially expressed genes at upregulation (A) and only seen in the treated samples (B). The line color indicates the type of interaction evidence, and the line thickness indicates the strength of data support. The node color indicates enrichment of the reactome pathway of proteins. Edges represent meaningful protein−protein associations.

Table 1. Summary of the Identified Hub Genes Implicated in the Apoptogenic Molecular Mechanisms of IDH1-Mutant High-Grade Gliomas

glucose homeostasis	cholesterol homeostasis	Ca^{2+} homeostasis	signal transduction	protein folding	transcriptome regulation and neurogenesis	cell adhesion, migration, and organization
ALDH ↑	VIM ↑	ANXA1 ↑	GNAQ+	PSMD5 +	LMNA↑	ICAM1+
AOC+	AP2A2 +		RRAS2+	PSMF1+	HIST ↑	EZR+
GSS+	AP2A1 +		RRAAS+	SEL1L+	MAPK1 ↑	RDX +
MAOB ↑	AP2B1+		RAB1A ↑	NPLOC4 +	NAP1L4+	
GRHPR+	AP1B1+		SCRN1 ↑		VIM ↑	
PEA-15 ↑	ERLIN2 +		GDI2 ↑		SPTAN1 ↑	
GSTM2+	ERLIN1+		CD44 ↑		PEA-15 ↑	
CKB ↑					TMEM43 ↑	
PYGB ↑					TRA2B +	
					SYNCRIP +	
					H2AFX ↑	
					H3F3A +	

+ Genes only expressed in the treated neurospheroids; ↑upregulated genes.

renewal with expression of stemness gene markers of VIM, Nestin, CD44, GFAP, IDH1, and βIII-tubulin, which were confirmed by proteomic analysis.

Histological staining adopted in our protocol has allowed target validation and visualization of tumor proliferation throughout spheroid sections. It was also suitable for the assessment of cytotoxic responses following pesticide treatment (Figure 3).

Effects of Pesticide Mixture on Tumor Stem-like Cell Proliferation and Viability

The results have shown that the viability and proliferation of spheroids consecutively decreased over the treatment concentrations. This proves that pesticides exhibit a neurotoxic effect to mitigate cell density proliferation with the gradual appearance of apoptotic and necrotic cells.

Proteomics Analysis

Cancer cells evade mechanisms which normally regulate metabolic programs in order to survive, satisfy their biosynthetic needs of high energy, fuel their continuous cell growth, rapidly proliferate, and seed in secondary organs from the aberrant and reprogrammed metabolism.

The glycolytic flux feature preferred by cancer cells represents the Warburg effect, defined as the aerobic energy production by glycolysis in which pyruvate is largely converted to lactate and secreted, rather than oxidative phosphorylation in normal tissues.[62,63] Thus, the metabolic profile of cancer cells often includes an increased consumption of glucose and glutamine, high rates of glycolysis, and lactate fermentation with changes in the use of metabolic enzyme isoforms. Another important metabolic hallmark of cancer cells is the deregulation of the lipid

https://doi.org/10.1021/acs.jproteome.3c00395
J. Proteome Res. 2023, 22, 3534−3558

metabolism. GMB tends to show enhanced *de novo* fatty acid (FA) synthesis with increased lipid uptake and lipolysis to fuel its growth.[64−66] Moreover, the accumulation of lipid droplets in cancer cells acts as a pivotal adaptive response to harmful conditions. This elevated lipogenesis is also a feature directly correlated with both enhanced glucose and glutamine metabolism.[67] Malignant gliomas were also characterized by their increased prostaglandins and formed thromboxanes compared to MNGs and normal brains, which may influence calcium-ion levels.[68,69] The cross-talk between altered metabolisms with the tumor microenvironment can strongly impact other cancer hallmarks and signaling pathways to facilitate the tumorigenic process and define resistance to different therapies which happen by mutations of oncogenes and tumor suppressor genes to promote inflammation,[70] enhance angiogenesis,[71] drastically effect stromal cells, and even escape from the immune system.[72]

Three top canonical pathways, namely, acute phase response signaling, caveolar signaling, and calcium signaling, are involved in the physiopathology of tumors. The acute phase is a set of inflammatory responses initiated by immune cells within the tumor microenvironment. Endocytosis regulates tumor metastasis by the internalization of cell-surface receptors via pinocytosis, phagocytosis, or receptor-mediated endocytosis, the latter of which includes clathrin, caveolae, and nonclathrin or caveolae-mediated mechanisms. Then, progress for sorting and routing of cargo ends in lysosomal degradation, recycling back to the cell surface, or secretion. Multiple endocytic proteins are dysregulated in cancer to promote tumor metastasis, particularly migration and invasion.[73]

In our study, by proteome-wide profiling and mapping, accessing protein expression patterns between treated and nontreated neurospheroids, we revealed that the majority of identified proteins were key members implicated in glioma pathogenesis, found to be relevant to cellular metabolic processes and biological regulation, involved in binding, catalytic, and structural molecule activity. Afterward, by mapping functional networks, with the enrichment analysis, we revealed that the top signaling pathways involved in the mechanism of apoptogenesis were mainly related to the mitochondrial energy metabolism and redox regulation by the EGFR/PI3K/AKT/SREBP-1 signaling pathway, protein folding and degradation by the heat shock response/ubiquitin/proteasomal pathway, cell structure and neuronal growth by the MAPK/ERK signaling pathway, excitotoxicity by calcium-ion export signaling, signal transduction by both Wnt and GnRH signaling pathways, hematopoiesis, and inflammatory mediation by chemokine and cytokine signaling pathways.

Herein, we provide a bird's eye view of each altered pathway with the precise role of each identified candidate protein/gene in order to help in better elucidation of the apoptogenic mechanism and designing favorable therapeutic interventions.

Potential Pathways Affected by the Selected Pesticide Mixture

Mitochondrial Dysfunction with Impaired Energy Production. Reactome pathway analysis revealed that the commonly expressed proteins were associated with lipid metabolism, glycolysis, and TCA cycle, which are all of crucial importance to energy generation. Mitochondrial adenosine triphosphate (ATP) production is the main energy source of intracellular metabolic pathways.[74] It is not only synthesized and stored in nerve terminals, glial, and postsynaptic target cells but also acts as a ubiquitous signaling pathway that is released in response to neuronal activities and other stimuli (e.g., inflammation, cellular damage). Besides, it modulates synaptic transmission between glial cells and neurons.[75] It is also involved in protein folding and the inhibition of aggregation and destabilization.

From a literature review, pesticides from neonicotinoids and pyrethroid classes can bind to macromolecules and intracellularly cause oxidative stress by the net production of ROS, especially in mitochondria, which can result in the onset of cell dysfunction. Proteins as one of the major targets of oxygen free radicals and other reactive species may encounter post-transitional modifications (PTMs) that affect a variety of its cellular functions.

The most commonly described metabolic proteins implicated in oxidative stress are enolases, (ENO1, ENO2), phosphate dehydrogenases (G3PDH), aldolases (ALDOC), phosphoglycerate kinases (PGK1), aconitases (ACO), and malade deshydrogenases (MDH2). Herein, diverse proteins involved in energy metabolism have been identified including the upregulation of the aldehyde dehydrogenase family (ALDH1A1, ALDH1A3, ALDH1B1, ALDH2, ALDH1A2), transferase (CKB), amine oxidase (MAOB), prenylcysteine oxidase (PCYOX1), glycogen phosphorylase (PYGB) that is located predominantly in the brain, and adaptor protein-15 of proliferation and apoptosis (PEA-15), which regulates glucose transport by controlling both the content of SLC2A1 glucose transporters in the plasma membrane and the insulin-dependent trafficking of the solute carrier SLC2A4.[34]

Five other proteins were only expressed in the treated spheroids, namely, amine oxidases (AOC2, AOC3), oxidoreductases (CRYL1, GRHPR), glutathione synthetase (GSS), glutathione S-transferase mu-2 (GSTM2), and hydrolases (PHPT1).

Proteins encoded by ALDH, MAOB, AOC, GRHPR, PEA-15, GSTM2, and GSS were considered key candidates as they exhibit strong relationships in the PPI network.

The identified downregulated proteins include enolases (ENO1, ENO2) as key glycolytic enzymes, which, beyond their glycolytic and gluconeogenic activities, are implicated in a variety of regulatory functions associated with hypoxia and ischemia; phosphoglycerate kinase (PGK1), implicated in ATP production via glycolosis; glyceraldehyde-3-phosphate dehydrogenase (GAPDH); NADPH-dependent reductase (CBR1) that catalyzes reduction of a wide range of carbonyl compounds involved in neuroprotection against oxidative stress; lactate deshydrogenease (LDH); isocitrate deshydrogenase-1 (IDH1), involved in the control of oxidative cellular damage; superoxide dismutases (SOD1, SOD2), which are mainly involved in ROS detoxification within the mitochondrion; aldolase (ALDOC), as a glycolytic enzyme expressed specifically in the hippocampus and Purkinje cells of the brain; and ADP ribosylation factor like GTPase-6 interacting protein-5 (ARL6IP5), which regulates the intracellular concentrations of taurine and glutamate and negatively modulates the SLC1A1/EAAC1 glutamate transport activity by decreasing affinity for glutamate in a Protein kinase C (PKC) activity-dependent manner.[34] All of the solute carrier (SLC) family drug transporters were found to be downregulated, which is similar to the effects of allethrin and tetramethrin pyrethroids reported to inhibit various ABC, SLC drug transporters, and organic anion transporters (OATs).[76]

Studies on U87MG cells had revealed high expression levels of proteins involved in ROS detoxification as prognostic factors for

https://doi.org/10.1021/acs.jproteome.3c00395
J. Proteome Res. 2023, 22, 3534−3558

tumor progression associated with a short median survival.[77] Also, tumor-produced lactate concentrations were reported with shorter survival and increased metastases.[78−80] Thus, the loss of functions of the above-cited metabolic enzymes impairing glucose metabolism may result in accumulation of glycolytic intermediates, which could be a target for an anticancer effect.

Other identified proteins were involved in the deregulation of the lipid metabolism such as VIM mediating neuritogenesis and cholesterol transport, hydroxyacyl-CoA dehydrogenase subunit β (HADHB), adaptor-related protein complexes (AP2A1, AP2A2, AP2B1, AP1B1), ER lipid raft (ERLIN2, ERLIN1), α chain of the antigen-presenting major histocompatibility complex (HLA-DRA), Cullin-associated and neddylation-dissociated-1 (CAND1), cytochrome b5 (CYB5B), complement factor H-related-1 (CFHR1), and prosaposin (PSAP). The role of each encoded protein is described in Supplementary Table S4.

In the PPI networks, APs were found to be key candidate genes showing strong connections to each other and implicated in the biological process of a low-density lipoprotein particle receptor catabolism. The two proteins encoded by ERLIN1 and ERLIN2 were strongly connected to each other and are involved in cellular cholesterol homeostasis regulation by the SREBP signaling pathway. The EGFR/AKT/SREBP signaling regulates GMB growth and survival by upregulating the transcription factor sterol regulatory element-binding protein (SREBP-1), which controls cholesterol synthesis, and the low-density lipoprotein receptor (LDLR), which mediates cholesterol uptake and the lipid metabolism.[81,82] Studies *in vitro* had shown that the downregulation of SREBP-1 inhibited cell proliferation and induced apoptosis in both HepG2 and MHCC97L cells;[83] consequently, SREBP-1 could be a promising target for treating grade-IV astrocytomas.[84,85] The downregulation pattern of lipid metabolism induced by our pesticide molecules was similar to the effects of the OP azathioprine to antagonize the aberrantly elevated lipid metabolism by blocking the EGFR/AKT/SREBP-1 signaling leading to GBM cell apoptosis.[81]

Both AP2 and ERLIN have shown strong relationships with other proteins implicated in cell structure, signal transduction, and protein folding, which enhances the role of the lipid metabolism in the regulation of numerous cellular homeostasis such as cell growth, proliferation, differentiation, survival, apoptosis, chemotherapy response, and drug resistance.

Collectively, our study suggests that the pesticide mixture led to endoplasmic reticulum (ER) oxidative stress-mediated apoptosis affecting proteins related to glycolysis, the TCA cycle, and lipid metabolism by blocks of cholesterol intake and synthesis, which may account for the impaired energy metabolism considered as a primary cause of chemioresistance.[86]

Protein Folding. The ER serves many functions, including assembly, folding, PTMs, and protein transport. In addition, it stores the calcium required for muscle contraction. ER stress occurs whenever the protein folding capacity is overwhelmed. Cells that undergo ER stress are characterized by the accumulation of misfolded proteins inside the ER lumen. A group of identified genes, including SEL1L, PSMF1, PDIA3, CCT, STIP1, NPLOC4, PSMD5, and HSP90AA1, were relevant to protein folding. PDIA3 modulates the folding of newly synthesized glycoproteins with disulfide isomerase activity to ensure the correct folding of secreted proteins. Its neuroprotective roles against toxicity and ß-amyloid aggregation in Alzheimer's disease have been documented.[87] The heat shock proteins (HSPs) are induced in cells exposed to stress and function as molecular chaperons involved in protein folding.[88] Namely, HSP90 and cytoplasmic chaperonin including TCP-1 (CCT) use the energy derived from ATP binding and hydrolysis to carry out their actions, such as stabilizing non-native proteins, transporting misfolded proteins to the proteasome, as well as providing conditions that are favorable for protein folding.[34] The activity modification of these proteins in the heat shock response/ubiquitin/proteasomal pathways related to the downregulation of cytoskeletal proteins results in growth arrest and reduced levels of actin and tubilin, aberrantly folded proteins, and hence inclusions containing ubiquitinated proteins (protein aggregation) that are implicated as one of the pathogeneic mechanisms of neurotoxicity in Alzheimer's disease, amyotrophic lateral sclerosis, and Parkinson's disease.[89]

Stress-induced phosphoprotein-1 (STIP1) acts as a cochaperone for HSP90AA1, while non-ATPase-5 (PSMD5) acts as a chaperone during the assembly of the 26S proteasome. The proteasome inhibitor subunit 1 (PSMF1) plays an important role in controlling the proteasome function.[34]

SEL1L, expressed only in treated cells, is an adaptor subunit of ERAD E3 involved in the ubiquitin-dependent degradation of misfolded ER proteins.[34] It enhances Synoviolin 1 (SYVN1) stability, which removes unfolded proteins, accumulated during ER stress, by retrograde transport to the cytosol from the ER.[34] This protein also uses the ubiquitin-proteasome system for the additional degradation of unfolded proteins. The ternary complex containing the ubiquitin recognition factor in ERAD (UFD1), the valosin containing protein (VCP), and the ubiquitin recognition factor (NPLOC4) binds ubiquitinated proteins and plays a crucial role in the export of misfolded proteins from the ER to the cytoplasm, where they are degraded by the proteasome.[34] All of PSMD5, PSMF1, SEL1L, and NPLOC4 are key candidate genes strongly connected in the PPI networks.

Cytoskeleton, Intermediate Filament Organization, Transcription Regulation, and Neurogenesis. We have identified upregulated proteins involved in binding, cytoskeleton structure, and transcription regulation such as the family of histones (HIST1H, HIST2H, HIST3H, H2AFX), lamins (LMNA), mitogen-activated protein kinases (MAPK1), member RAS oncogene family (RAB1A), proline- and arginine-rich end leucine-rich repeat protein (PRELP), reticulon 4 (RTN4), PEA-15, spectrins (SPTAN1), transmembrane protein-43 (TMEM43), tubilins (TPPP3), and vimentin (VIM). The other involved proteins generated in the treated spheroids were ezrin (EZR), cysteine- and glycine-rich protein-1 (CSRP1), intercellular adhesion molecule (ICAM1), inner membrane mitochondrial protein (IMMT), nucleosome assembly protein 1-like (NAP1L4), radixin (RDX), regulator of transcription (SUB1), septin (SEPT8), and twinfilin actin-binding protein-1 (TWF1), transformer-2-β homolog (TRA2B), and synaptotagmin binding cytoplasmic RNA-interacting protein (SYNCRIP).

DNA accessibility is regulated via a complex set of histone PTMs and nucleosome remodeling. Histones are necessary for the condensation of nucleosome chains into higher-order structured fibers and act as regulators of individual gene transcription through chromatin remodeling, nucleosome spacing, and DNA methylation.[34] Thereby, histones play a central role in transcription regulation, DNA repair, DNA replication, and chromosomal stability. They were identified as key proteins, exhibiting strong links together as well as to other

https://doi.org/10.1021/acs.jproteome.3c00395
J. Proteome Res. 2023, 22, 3534−3558

relevant proteins implicated in the same biological process such as protein encoded by NAP1L4, which acts as a histone chaperone in nucleosome assembly, and Lamins that play a crucial role in nuclear assembly, chromatin organization, nuclear membranes, and telomere dynamics, required for the normal development of the peripheral nervous system and muscle satellite cell proliferation.[34]

The mammalian family of MAPKs activated by diverse stimuli such as hormones, oxidative stress, and ER stress mediates intracellular signaling associated with a variety of cellular activities such as proliferation, differentiation, survival, and death. These MAPK pathways include ERK, p38, and c-Jun NH(2)-terminal kinase (JNK), with each signaling consisting of at least three components, an MAPK kinase kinase (MAP3K), an MAPK kinase (MAP2K), and an MAPK. Both MAPK1/ERK2 and MAPK3/ERK1 play a crucial role in the MAPK/ERK cascade involved in several steps of tumor development[90] and in the expression of matrix metalloproteinases promoting degradation of extracellular matrix proteins and subsequently tumor invasion.[90] The protein encoded by the RAS is involved in the regulation of the MAPK signaling pathway. The PEA-15 enriched in astrocytes blocks the Ras-mediated inhibition of integrin activation and modulates the ERK/MAPK cascade.[34] The involved roles of the other identified proteins are explained in Supplementary Table S4.

Microtubules are dynamic cytoskeleton polymers mediating essential functions such as axon, dendrite growth and neuron migration throughout brain development.[34] Tubilins are the major components of microtubules performing as regulators with binding activities.[34]

From the PPI networks, all of LMNA, HIST, H2AFX, MAPK1, and PEA-15 are hub genes strongly related to each other, likewise for ICAM1, EZR, and RDX and for TRA2B and SYNCRIP.

The extensive VIM expression has been postulated as a molecular marker for highly infiltrative gliomas with poor prognosis,[91] which is our case study found at a higher expression level.

The other involved genes identified at downregulation are DPYS (dihydro-pyrimidinase), necessary for cytoskeleton remodeling; TUB (tubulin superfamily TUBA, TUBB); PTRF (caveolae-associated protein-1), implicated in caveolae organization, RNA binding, and transcriptional regulation in response to metabolic challenges; MTHFD1 (methylene-tetrahydrofolate dehydrogenase), encoding a protein with enzymatic activities to catalyze substrates for methionine, thymidylate, and *de novo* purine syntheses; and CFL1 (Cofilin1), required for neural tube morphogenesis, neural crest cell migration, cell morphology regulation, and cytoskeleton organization.[34]

Excitotoxicity. Calcium signaling is crucial for several aspects of plasticity in glutamatergic synapses. It acts as a secondary messenger and regulates various cellular processes by calcium-modulated proteins. We have notably observed some altered calcium-binding proteins such as calcium transporters, sensors, regulators, and effector proteins, reported to be differently expressed in tumor progression and metastasis and implicated in the deregulation of calcium homeostasis in GBM.[69] The calcium-regulatory proteins include several isoforms of S100 calcium-binding proteins (A10, A11, A12, A6, A8, A9, and B), annexins (ANXA2, ANXA4, ANXA5, ANXA6, and ANXA7), integrins (ITGB2, ITGAM), and others, such as cysteine-rich acidic matrix-associated protein (SPARC) and calumenin (CALU). Other proteins involved in calcium signaling include glutathione synthetase (GSS) and the serpin superfamily (SERPINA1, A3, B1, B6, C1, F2, G1, H1).

S100A4 interacts with not only tropomyosin (TPM4), implicated in the stability of filaments and other acting-binding proteins, but also with myosins (MYH9), involved in cytokinesis, cell motility, and cell shape maintenance, thus suggested to affect the cytoskeleton of the tumor cells.[69,92] The complex formed between ANXA2/S100A10 and the nucleoprotein AHNAK was reported to regulate the actin cytoskeleton and cell membrane architecture.[93] Changes in the calcium-related proteins and their interactors imply cytoskeletal changes, leading to tumor cell proliferation and metastasis in a calcium-dependent manner.

Proteases from the serpin superfamily are highly expressed in glioma tumors.[94] They are involved in calcium homeostasis. A novel study conducted by Godinez et al. (2022) has revealed that neuroserpin plays an important role in mediating neurite outgrowth and axonal development as well as in maintaining normal synaptic plasticity through its inhibitory effects on the tissue plasminogen activator (tPA) in the CNS, thereby preventing tPA interaction with the NMDA receptor-mediated calcium influx, which contributes to excitotoxic neuronal apoptosis.[95,96] The elevated expression of serpin superfamily proteins was associated with low survival and increased recurrence rates.[97]

Another identified protein encoded by CAMK (2A, 2B, 2D) is a member of the *N*-methyl-D-aspartate receptor (NMDAR) signaling complex in excitatory synapses regulating the NMDAR-dependent potentiation of the AMPA receptor and therefore excitatory synaptic transmission.[34] It acts autonomously after ca^{2+}/calmodulin binding and autophosphorylation and is involved in synaptic plasticity, neurotransmitter release, and long-term potentiation. It also regulates the migration of developing neurons and phosphorylates the transcription factor FOXO3 to activate its transcriptional activity.[34]

The roles of other identified proteins are explained in Supplementary Table S4. In contrast to studies on U87MG, revealing the overexpression of Ca^{2+} binding proteins,[98] our involved proteins in calcium signaling were found downregulated. The overall effects suggest that calcium homeostasis and signaling deregulation in tumor cells were affected by pesticide treatment.

Signal Transduction. For cell proliferation, differentiation, and growth, the most implicated proteins identified in our study were RAS related (RRAS), GDP dissociation inhibitor-2 (GDI2), transducer G protein (GNAQ, GNB2, GNB4), secremin-1 (SCRN1), transforming growth factor-β-induced (TGFBI), CD44, ATPase/H+-transporting-V1-subunit-A (ATP6 V1A), and tyrosine 3-monooxygenase/tryptophan 5-mono-oxygenase activation protein zeta (YWHAZ). The roles of these identified proteins are explained in Supplementary Table S4.

Both GNAQ and RRAS yielded only in the treated samples, where hub genes strongly related to each other in a single module. The genes TGFBI, YWHAZ, and ATP6 V1A, frequently upregulated in tumor cells, were found downregulated by our pesticide treatment. The other identified proteins at upregulation include GDI2, GNB2, GNB4, SCRN1, and PEA-15, which inhibit the TNF receptor superfamily (TNFRSF6 and TNFRSF1A)-mediated Casp-8 activity and apoptosis, and the GTPases Rab family, which are key regulators of intracellular membrane trafficking, among which RAB1A regulates vesicular protein transport from the ER to the Golgi

https://doi.org/10.1021/acs.jproteome.3c00395
J. Proteome Res. 2023, 22, 3534−3558

compartment and plays a crucial role in cell adhesion and cell migration.[34] Both RAB1A and GDI2 are key candidate genes.

Hematopoeisis. Tumor progression is associated with profound perturbations in hematopoiesis. Angiogenesis plays a critical role in their growth. Based on PPI network analysis, some identified proteins, especially the downregulated ones, were involved in blood vessel remodeling (blood coagulation) and platelet degranulation. F13A1 encodes the coagulation factor XIII protein, which is an acyl transferase involved in a blood coagulation cascade, activated by thrombin and calcium ions to a transglutaminase. The latter catalyzes cross-link formation between fibrin chains, stabilizing the fibrin clot.[34] F13A1 was found at a highly altered activity, which may lead to extensive cross-linking and aggregation described in many neurological disorders. Another altered protein encoded by PGK1 and secreted by tumor cells is involved in angiogenesis by reducing disulfide bonds in the serine protease plasmin, which consequently leads to the release of the tumor blood vessel inhibitor angiostatin.[34] ENO1 beyond its glycolytic activity was also reported to alter plasminogen and plasmin activity.[99]

Other Identified Proteins. Several identified downregulated proteins were key members implicated in glioma pathogenesis or described as predictors of tumorigenicity, e.g., prohibitin (PHB2); glial fibrillary acidic protein (GFAP), as a member of the class-III intermediate filament proteins of mature astrocyte (Grade III); chitinase 3 like 1 (CHI3L1), also called YKL-40, which promotes activation of VEGF expression and induces new tumor vasculature;[100,101] erythrocyte membrane protein (EPB41L), implicated as a tumor suppressor; scavenger receptor B2 (SCARB2); ATP-dependent DNA helicase II (XRCC6), also named KU-70, which is a DNA repair protein with helicase activity; CD163 expressed by tumor-associated macrophages;[102] integrins (ITGB2, ITGAM), as cell-surface glycoproteins participating in cell adhesion and cell-surface-mediated signaling;[34] cystatin (CSTB, CST3) and cathepsins (CTSB, CTSD), which may facilitate tumor invasion and metastasis in glial cells in an imbalance state;[103,104] intermediate filament and actin-binding proteins, as GFAP and FSCN1 (fascin actin-bundling protein-1), which mediate reorganization of the actin cytoskeleton and axonal growth cone collapse in response to the nerve growth factor; calponin-3 (CNN3), as a thin filament-associated protein capable of binding to actin, calmodulin, and tropomyosin; and capping actin-protein (CAPG), which plays a pivotal role in regulating nuclear structures through potential interactions with actin.[34]

There are two other types of proteins involved in the translation process: translation initiation factors (EIF3G, EIF4A1, EIF4A2, and EIF5A) and elongation factors (EEF1A1, EEF1A2, EEFD, EEFG, and EEF2). The roles of these proteins are described in Supplementary Table S4.

Some neural markers have been identified, namely, SLC25A (solute carrier family 25), which are gated pores through which ADP is moved across the cytoplasm into the mitochondrial matrix and ATP is moved from the mitochondrial matrix into the cytoplasm.[34] Nestin (NES) is an intermediate filament protein that together with VIM is a marker of highly aggressive and metastatic forms of cancer, attributed to the growing grade malignancy.[105] Our results correlate well with those of other studies showing the higher expression levels of VIM in gliomas treated by Temozolomide even when applied with irradiation.[106]

In the glioma microenvironment, astrocytes could increase the IL-6 secretion and stimulate the expression of membrane type-1 matrix metalloproteinase (MT1-MMP or MMP14). The latter is a proteolytic enzyme involved in extracellular matrix degradation and assists in cancer invasion and progression;[107] also, the same role is found for the identified genes MMP8 and MMP9.[108] Isoforms S100A and S100B are considered potential biomarkers for glioma classification and prognosis.[69,109] The mutational status of the immunoglobulin heavy variable (IGHV) is also quite frequently studied in relation to cancer.[110]

Expression of the gonadotropin-releasing hormone (GnRH) and its receptor has been reported to be expressed in several tumors including gliomas. GnRH agonists have shown an inhibitory effect on cell invasion and cell proliferation in various cancer cell lines (e.g., Zoladex). Indeed, a recent study carried out by Tripathi PH. et al. (2022) has revealed an overexpression of a cysteine proteinase inhibitor, KNG1, that inhibits cell proliferation and angiogenesis in response to GnRH agonists in glioma cells. This inhibition was also related to the breakdown of EGFR/PI3K/AKT signaling,[111,112] assuming a likely strong link between GnRH and EGFR signaling pathways via KNG1. In contrast, in our study, both KNG1 and lactotransferrin isoform 2 (LTF), preventing cancer development and metastasis, were downregulated. This could be explained by a negative feedback mechanism, associated with the upregulation of Gnb4, Gnb2, and PEA-15 involved in the GnRH signaling pathway as modulators. These genes exhibited strong relationships together in a module related to MAPK1 enhancing its activity. In fact, the three major classes of MAPKs, namely, ERK, JNK, and p38, were demonstrated to be activated following GnRH receptor occupancy in pituitary gonadotropes,[113] especially the ERK1 isoform involving Ca^{2+} release in PKC-dependent or -independent pathways.[110] Another study by Feixue Li had also shown that cypermethrin disrupted Ca^{2+} homeostasis by both influx of extracellular Ca^{2+} through L-type voltage-gated calcium channels and release from ER via inhibition of Ca^{2+}-ATPase, resulting in the activation of PKC/c-Raf/ERK1/2/gene pathways with a subsequent increase in the transcription of gonadotropin subunit genes.[114]

Although the underlying molecular mechanism remains ambiguous since the interaction of pesticides with hormone receptors is confusing, our finding may reveal that grade-IV astrocytomas promote the downstream of the MAPK1/ERK2 pathway involving the massive Ca^{2+} influx. Furthermore, the GnRH signaling-enhancing MAKP activities likely serve as negative feedback compensatory regulators that modulate MAPKs and EGFR signalings.

Although the presence of IDH mutations predicts a favorable disease outcome,[8] our finding revealed that the MAPK/ERK cascade and EGFR play a prominent role in the astrocytoma high-grade invasiveness, in which patients exhibited altered expressions of KNG1 and LTF, compatible with a poorer prognosis and lower survival rates following previous studies.[111,112] Thus, MAPK and EGFR in the GnRH signaling pathway implicated in the regulation of cell proliferation, differentiation, survival, and death could be well-investigated for cancer therapy.

In summary, based on a comparative analysis of proteome profiles under stressful conditions, we succeeded in identifying the prognostic biomarkers and pivotal signaling pathways involved in IDH mutant high-grade gliomagenesis, which help to better understand and elucidate the molecular apoptogenic mechanisms and design favorable therapeutic interventions. In this context, candidate proteins associated with lipid metabolism, glycolysis, and the TCA cycle for the impaired energy

https://doi.org/10.1021/acs.jproteome.3c00395
J. Proteome Res. 2023, 22, 3534−3558

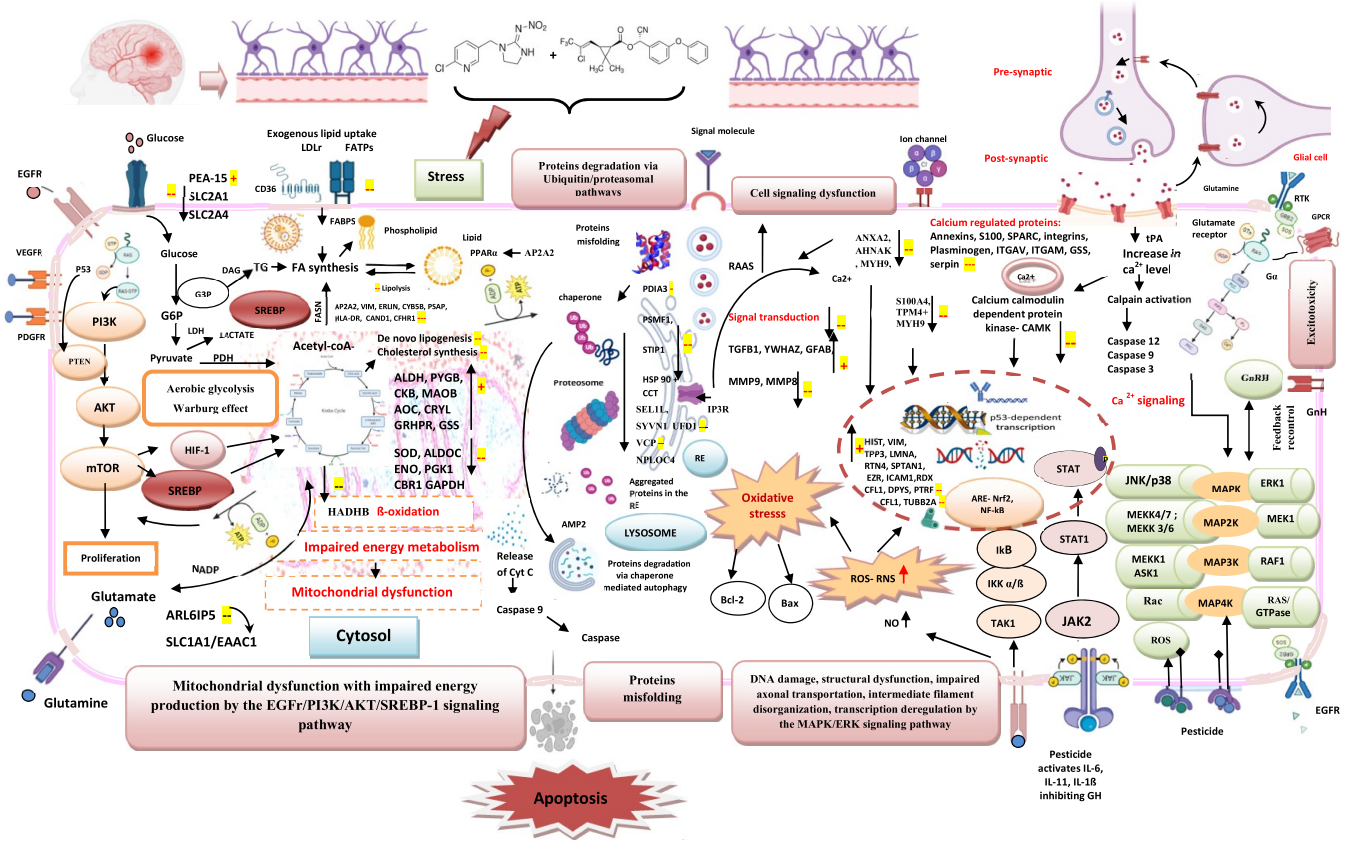

Figure 9. Schema outlines the potential signaling pathways affected by pesticide treatment with the differently identified expressed proteins involved in the anticancer action of IDH1-mutant high-grade gliomas. (1) Impaired energy metabolism and mitochondrial dysfunction by the EGFr/PI3K/AKT/SREBP-1 signaling pathway: Oncogene mutation of Ras/GTPases activates mTOR via the PI3K-AKT-mTOR signaling pathway, which indirectly affects other metabolic pathways by activating HIF-1. Consequently, proteins related to glycolysis, the TCA cycle, and lipid metabolism were found to be altered by ER oxidative stress induced by pesticide treatment. (2) Protein disfolding degradation by the heat shock response/ubiquitin/proteasomal pathway. (3) Structural dysfunction, impaired axonal transportation, neuritic abnormalities, DNA damage, and impaired neuronal communication by the MAPK/ERK signaling pathway: MAP3Ks, which are activated by MAP4Ks or GTPases, mediate the phosphorylation and activation of MAP2Ks, which in turn phosphorylate and activate MAPKs. Activated MAPKs phosphorylate various substrate proteins including transcription factors, resulting in regulation of a set of cellular activities, namely, cell proliferation, differentiation, migration, inflammatory responses, and death. The mammalian MAPK gene family converges signals from G protein coupled receptors (GPCRs) or growth factor receptor-tyrosine kinases (RTKs), then via an adaptor molecule GRB2, and a guanine nucleotide exchange factor, mSOS, to activate the small GTP-binding protein, Ras, followed by activation of the MAPK cascade. The MAPK family includes ERK, p38, and JNK. In the ERK signaling pathway, ERK1/2 is activated by MEK1/2, which is activated by Raf. This latter is activated by Ras GTPase. In p38 signaling, the TNF receptor-associated factor (TRAF) activates ASK1, TAK1, or MEKK1, which activates MKK3/6, and then MKK3/6 phosphorylates p38 isoforms. In JNK signaling, RAC1 activates MEKK1 or MEKK2/3 to activate MKK4/7, and then, MKK4/7 phosphorylates JNK1/2/3. The ASK1 in the p38 signaling also activates MKK4/7 to cross-talk with JNK signaling. Ca^{2+} is required for MAPK/ERK pathway activation by the downstream of PKC and PTK signalings. (4) Pesticides may also mediate KEAP1/NRF2/ARE activation as well as the NF-kB signaling pathway responsible for cell defense against oxidative stress, with molecular cross-talk to the apoptosis-regulatory machinery through activation of the ASK1 kinase by a KEAP1 binding partner, PGAM5. (5) Cell signaling dysfunction by altering TGF-β and GnRH signaling pathways: pesticides may induce inflammatory cytokines (IL-6, IL11, IL-1ß) and caspases inhibiting growth hormone (GH) leading to endocrine disruption and activation of JAK2/STAT1 signaling. Phosphorylation of the C terminal of STAT1 enhances the activity of other factors such as p53; together with the action of DNA topoisomerase II, these molecules can cause DNA damage and eventually apoptosis. (6) Excitotoxicity: Pesticides disrupted Ca^{2+} homeostasis by influx of extracellular Ca^{2+} through L-type voltage-gated calcium channels, release from ER via inhibition of Ca^{2+}-ATPase, and activation of NMDA receptors of glutamine. Stimulation of calcium-dependent apotogenic signaling pathways ultimately results in an increase of the Ca^{2+} level, activation of calpain and caspases, and thus excitotoxicity and cell death. (7) Pesticide mixture increases the nitric oxide species (NOXs), which in turn increases RNS/ROS signaling, promoting oxidative stress in cells, which may induce lipid, protein, and DNA oxidation, resulting in mitochondrial dysfunction and apoptosis. Upregulation and downregulation of the differently expressed proteins identified in the treated neurospheroids are highlighted in yellow color. **AKT**, serine/threonine kinase; **AP2**, adaptor-related protein complexes; **ARE-Nrf2-NF-kB**, antioxidant-responsive element-nuclear factor-erythroid-2-related factor 2, nuclear factor-kappa light chain enhancer of activated B cells; **ASK1**, apoptosis signal-regulating kinase 1; **DAG**, diacylglycerol; **FABP**, fatty acid binding proteins; **FASN**, fatty acid synthase; **EGFR**, epidermal growth factor receptor; **ER**, endoplasmic reticulum; **FA**, fatty acid; **G3P**, glyceraldehyde-3-phosphate; **G6P**, glucose-6-phosphate; **GnrH**, gonadotropin-releasing hormone; **GH**, growth hormone; **GRB2**, growth factor receptor-bound protein 2; **HIF**, hypoxia-induced factor; **IP3R**, IP3 receptor; **IP3**, inisitol-3-phosphate; **JAK-STAT**, Janus kinase-signal transducer and activator of transcription; **JNK**, c-Jun N-terminal kinases; **KEAP1**, Kelch-like ECH-associated protein-1; **LDH**, lactate deshydrogenase; **MAPK/ERK**, mitogen-activated protein kinase/extracellular-signal-regulated kinase; **mSOS**, mammalin son of sevenless; **mTOR**, mammalin target of rapamycin kinase; **NMDA**, *N*-methyl-D-aspartate; **PLC**, phospholipase C; **PKC**, protein kinase C; **PDGFR**, platelet-derived growth factor receptor β; **PPAR**, peroxisome proliferator-activated receptor; **PI3K**, phosphatidylinositol-3-kinase; **PKC**, protein kinase C; **PTK**, protein tyrosin kinase; **PTEN**, phosphatase and Tensin homolog; **PDH**, pyruvate deshydrogenase; **PGAM5**,

https://doi.org/10.1021/acs.jproteome.3c00395
J. Proteome Res. 2023, 22, 3534−3558

Figure 9. continued

phosphoglycerate mutase 5; **RE**, reticulim endoplasmic; **ROS**, reactive oxygen species; **RNS**, reactive nitrogen species; **RTK**, receptor-tyrosine kinase; **SREBP-1**, sterol regulatory element-binding transcription factor 1; **TNF**, tumor necrosis factor; **TG**, triglyceride; **TGF**, transforming growth factor; **tPA**, tissue plasminogen activator; **VEGFR**, vascular endothelial growth factor receptor. Created by K. Louati.

metabolism were encoded by ALDH, AOC, MAOB, CKB, PYGB, GRHPR, PEA-15, GSTM2, GSS, APs, ERLIN, and VIM genes. In protein folding, SEL1L, PSMF1, NPLOC4, and PSMD5 genes were relevant. In transcriptome regulation and neurogenesis, LMNA, HIST, H3F3A, H2AFX, SPTAN1, VIM, TMEM43, TRA2B, SYNCRIP, NAP1L4, MAPK1, and PEA-15 were hub genes. In cancer-related cell adhesion, migration, and organization, ICAM1, EZR, and RDX genes were relevant. In the excitotoxicity mechanism, we identified proteins encoded by CAMK (2A, 2B, 2D), isoforms of S100 calcium-binding proteins, annexins, integrins, and proteases from the serpin superfamily. In signal transduction, GNAQ, RRAS, RAB1A, SCRN1, CD44, and GDI2 were key genes. In hematopoiesis, F13A1, PGK1, and ENO1 were relevant. Interestingly, Gnb4, Gnb2, and PEA-15 were involved in the GnRH signaling pathway as modulators enhancing the MAPK activity.

Our study highlights the relevance of each protein/gene with its meaningful relationships and regulations as well as the role of a feedback compensatory effect for some involved mechanisms.

Figure 9 illustrates all of the potential altered signaling pathways, with key involved genes/proteins and cross-talk linking mechanisms, as hallmarks of cancer biology for high-grade gliomas carrying IDH mutation.

Therapy Target Pathways for Human IDH Mutant High-Grade Gliomas

IDH mutations are among the earliest genetic events driving tumorigenesis.[8,9] Specific biomarkers released during tumor progression might be useful to specify the malignancy grade and serve as a specific target for treatment. Moreover, the identified altered signaling pathways by the proteomic study play crucial roles in anticancer action.

From a literature review, a wide variety of therapeutic strategies are adopted in gliomas, namely, direct approaches such as targeting the GSC signaling by blocking several pathways such as the Notch signaling, the Wnt/ß-catenin signaling, the sonic hedgehog (SHH) signaling, and the receptor-tyrosine kinase (RTK) signaling, including growth factor receptors (EGFR, PDGFR, VEGFR). The indirect approaches include targeting the perivascular niche via angiogenic pathways or the immune niche. However, challenges may persist such as the risk alteration in normal neural stem-like cells (NSCs) and progenitor cells.[52]

Targeting apoptogenic signaling pathways especially in tumors remains a promising strategy in oncology.[115] Apoptosis can be triggered by two different signaling pathways including not only extrinsic pathways such as modulation of death receptors, which in turn results in the recruitment of specialized adaptor proteins and activation of caspase cascades leading to apoptotic cell death, but also intrinsic pathways involving the mitochondria and DNA damage, both of which act as a specific mitochondrial complex I (NADH-dehydrogenase) inhibitor that impairs cellular respiration and ATP production and generates ROS-inducing oxidation of lipids and proteins, which consequently inactivates certain enzymes and alters a diverse array of cellular processes.[116−119]

ER-induced apoptosis occurs via three primary pathways, namely, the IRE1 (inositol-requiring enzyme 1)/ASK1 (apoptosis signal-regulating kinase 1)/JNK pathway, the caspase-12 kinase pathway, and the C/EBP homologous protein (CHOP)/DNA damage-inducible protein-153 (GADD153) pathways.[81] Studies in the literature have proposed perturbation of the ER homeostasis as a favorable target to induce cancer cell death in GLB[120−122] and interestingly by purine analogues as the OP azathioprine with cladribine and fludarabine.[122]

In humans, IDH1, IDH2, and IDH3 genes are the three isoforms of the IDH enzyme, participating in significant metabolic processes such as the Krebs cycle, glutamine metabolism, lipogenesis, and redox regulation.[8,9] IDH1 is particularly important in the brain. It promotes tumor progression and resistance by the oxidative decarboxylation activity through efficient fatty acid synthesis, $NADP^+$ production, glutamine catabolism, and ROS scavenging activities.[8,9] Therefore, targeting distinctive metabolic patterns such as blockage of the NAD^+ salvage pathway or inhibiting the antioxidant pathways as glutaminase activity and glutathione (GSH) *de novo* synthesis presents effective tools for IDH-mutated malignancies.[8,9,63,123] From our study, the PI3K/AKT pathway is found to be a powerful mechanism for the altered tumor cell metabolism by inhibition of the glycolytic capacity and the lipogenic machinery SREBP-1 or the use of 3-hydroxy-3-methyl-glutaryl-CoA reductase (HMGCR) inhibitors (statins or SREBP inhibitors), e.g., fatostatin and botulin were reported to have favorable results in inhibiting cell-tumor growth.[124,125]

The mutant IDH1 (R132H), in addition to the loss of its normal catalytic activity, gains the function of generating D-(R)-2-hydroxyglutarate (2HG) via α-KG (α-ketoglutarate) inhibition. This overproduction of 2HG in cancer cells inhibits histone and DNA demethylases, resulting in a hypermethylation phenotype, blockage of cellular differentiation, and alterations in the epigenetic status.[126] Thus, genome transcription and DNA are two main ways that occurred to a greater extent in the IDH-mutated gliomas that could also be specific targets in cancer treatment strategies. In this regard, λ-CYH was reported to interact with enzymes belonging to the purinergic system involved in the metabolism of extracellular nucleotides and nucleosides, such as adenosine triphosphate (ATP), to induce DNA damage.[28]

Pesticides may also induce inflammatory cytokines (IL-6, IL-1) and caspases, which inhibit the growth hormone (GH) leading to the phosphorylation of the C terminal of signal transducers and activators of the transcription 1 (STAT1) protein at residue 727 and enhancing the activity of other factors such as p53 inducing DNA damage via the JAK-STAT (Janus kinase-signal transducer and activator of transcription) signaling pathway, which is critical for both neuronal survival and cell death.[127] Hence, this pathway could be a potential target for glioma therapy.

GnRH agonists exhibit an inhibitory effect on cell invasion, migration, and cell proliferation.[108] Although molecular targets associated with the GnRH receptors are not well-studied in cancers, our selected pesticides by their estrogen-mimicking ability have shown activation of the MAPK pathways with an

https://doi.org/10.1021/acs.jproteome.3c00395
J. Proteome Res. 2023, 22, 3534−3558

inhibitory effect on cell proliferation. Thus, targeting MAPK and EGFR in the GnRH signaling pathway is a promising strategy for anticancer therapy. In fact, to induce neuronal apoptosis, some developed drug targets promote the JNK and p38 signaling involved in oxidative stress response by activation of the MAP3K/ASK1 pathway[90] and/or inhibition of the Ras-Raf-MEK-ERK pathway implicated in tumor development, e.g., sorafenib has been described as an efficient RAF inhibitor drug.[128]

The selected pesticides can lead to the nuclear factor-κB (NF-κB) pathway as well as to KEAP1/Nrf2/ARE (Kelch-like ECH-associating protein-1/nuclear factor-erythroid-2-related factor 2/antioxidant response element) pathway activation, which is one of the most important defense mechanisms against oxidative stress closely associated with cancer and tumerigenesis.[129] Nrf2 is highly expressed in IDH1-mutated tumors, endowed with antiapoptotic, antioxidative, anti-inflammatory, and proliferative properties, which contributes to tumor angiogenesis and cell survival in the hypoxic environment by promoting the hypoxia-inducible factor 1α (HIF-1α) and VEGF pathways.[9,130] Simultaneously, KEAP1-Nrf2 signaling may be modulated by a complex regulatory network, including PI3K/AKT, PKC, and MAPK with molecular cross-talk to the apoptosis-regulatory machinery through activation of the ASK1 kinase by a KEAP1 binding partner, phosphoglycerate mutase (PGAM5).[131,132] Thus, regulation of the KEAP1/Nrf2 axis might appear as a novel therapeutic strategy,[133] especially when taking into consideration a synergic effect to inhibit the synthesis of GSH mediated by the Nrf2 transcription factor in the antioxidant activity.

The high intracellular Ca^{2+} level induced by pesticides, either by influx from receptor/ion channels or by release from intracellular stores via activation of inositol trisphosphate (IP3) receptors, is a key element in the apoptotic signaling described by a number of calcium-dependent apoptosis pathways, e.g., massive Ca^{2+} influx may induce neuronal nitric oxide synthase (nNOS), further increasing the production of ROS/RNS (reactive nitrogen species), and thereby increasing oxidative stress in the brain, which may induce lipid, protein, and DNA oxidation and result in mitochondrial dysfunction as well as release of cytochrome C, which activates caspase-9- and caspase-3-mediated proteolytic cleavage of PKC, together resulting in apoptosis.[134] Calpains (CAPNS) as calcium-activated cysteine proteases have been implicated in apoptosis induction through activation of a number of molecules related to the apoptosis process such as caspase-12, BAX (Bcl2-associated X protein), and Bid (BH3 interacting domain death agonist). Calmodulin (CaM), by binding four Ca^{2+} ions, undergoes a conformational change to fix to its target site on CaM kinases and induce phosphorylation of the regulatory domain, which affects many downstream pathways controlling a variety of cellular functions.

Some molecules from the pyrethroid class were investigated regarding their anticancer effect, e.g., deltamethrin (DLM) was found to increase the Ca^{2+} level by inducing PLC-independent Ca^{2+} release from the ER and Ca^{2+} entry by nifedipine-sensitive channels, and it was proposed as an anticancer agent at low concentrations (5−10 μM) inducing calcium-dependent apoptogenic signaling pathways in OC2 human oral cancer cells.[135] Another study had also involved the anticancer activity of DLM in human GBM cells at concentrations of 20−60 μM by increasing the Ca^{2+} level inducing intrinsic pathways of apoptosis via activation of CaM-dependent protein kinase (CaMK2) pathways.[136]

However, there are plenty of contradictory studies in the literature describing the role of CaMK2 as both proapoptotic[137,138] and antiapoptotic.[139] On the one hand, it was revealed that an increased Ca^{2+} level resulting from ER stress induced expression of the FAS death receptor through a pathway involving (CaMK2γ) and JNK. It was also shown that CaMK2γ induced mitochondrial-dependent apoptosis by release of cytochrome c and loss of the mitochondrial membrane potential. On the other hand, researchers have highlighted the role of CaMK2 in cancer development, cell migration, invasiveness, and metastasis development.[139]

In our case study, CaMK2 was downregulated, which could be assigned as a prognostic indicator of the high-grade astrocytomas. Indeed, He and Li have reported the role of CaMK2γ as a potential candidate for predicting GBM prognosis, wherein the altered transcript level was closely associated with the tumorigenesis and recurrence of high-grade gliomas compared to low-grade astrocytomas.[140] They also described the involvement of CaMK2 in regulating the stemness of GBM cells and that the altered activity of CaMK2γ not only abolished the stem-like traits such as cell growth and neurosphere formation but also the protein levels of GSC stemness markers, such as CD133, Nanog, Sox2, and Oct4.[140] Moreover, they showed that CaMK2γ was involved in therapeutic resistance and that it was found at overexpression enhancing the chemoresitance of liver cancer cells to 5-fluorouracil and ovarian cancer cells to cisplatin.[140]

Although the role of CaMK2 in cancer remains ambiguous as seen from the contradictory studies, there is maximum evidence from informatics analysis describing its critical role in cancer development, metastasis, resistance, recurrence, and sustentation of GSC stemness markers. Thus, CaMK2 may be a novel promising approach for the IDH mutant high-grade glioma therapy, e.g., calmodulin inhibitors were reported to trigger the proteolytic processing of membrane type-1 metalloproteinase to a bound-inactive form and enhance tissue inhibitors of MMP expression levels, resulting in a loss of migratory potential of U87MG cells.[141]

Based on our findings, we can suggest other straightforward therapeutic strategies to counteract the growth of IDH mutant high-grade gliomas, such as inhibition of the neuroserpin effect, which mediates in correlation with p63, tumor growth, metastasis, and cellular survival; likewise, the activation of the plasmin proteolytic axis was involved in multiple metastatic-suppressive mechanisms, in particular, degradation of the axonal path-finding L1 cell-adhesion molecule (L1CAM) specifically expressed by metastatic cancer cells during their invasion of the brain parenchyma and capillaries.[95]

Moreover, the increased expression of cystatins involved in apoptosis regulation elicited by oxidative stress is an attempt to counteract the autolytic properties of cathepsin(s). Thus, disturbing the balance between cystatin and cathepsin with targeted therapy can promote tumor cell death.[142,143]

Taking another attractive action, proteins encoded by the HSP90 (B1, AA1) family were found altered by pesticide treatment in the same way as the use of HSP90 inhibitors such as 17-N-allyl-amino-17-demethoxy-geldanamycin (17-AAG). Consequently, alteration of the chaperoning function, which induces the degradation of HSP90's client proteins,[144] could also be a potential therapy target for high-grade gliomas.

https://doi.org/10.1021/acs.jproteome.3c00395
J. Proteome Res. 2023, 22, 3534−3558

Interestingly, inhibitors of PI3K-mTOR and PLCγ,[145] and mediating the balance between antiapoptotic (BCL2 and BCL-XL) and proapoptotic proteins, were reported to be validated targets in tumor growth, invasion, and angiogenesis.[146−148] Hence, they could also be vulnerable targets in our case study of the IDH mutant high-grade gliomas.

CONCLUSIONS

The use of cell-culture models with proteomic-based approaches has increased over the recent years in cancer-related fundamental science research due to the recent advances in MS-high-throughput technology and the development of sophisticated bioinformatic tools with powerful algorithms of protein search databases, which have facilitated proteome-wide profiling and mapping with exquisite precision and accuracy.

In our study, by adopting an untargeted proteomic-based high-resolution MS/MS approach for differential proteome profiling analysis under stressful conditions, we have succeeded in identifying the prognostic biomarkers and pivotal signaling pathways involved in IDH mutant high-grade gliomagenesis. Hence, we have proved that the 3D-neurospheroid differentiation has recapitulated the important features of the neural target tissue, constituting a more accurate *in vitro* cell model for drug screening and development, relative to traditional 2D monolayer systems when addressing microenvironment remodeling in healthy and disease states, without the confounding effects of exogenous matrices.

Our data analysis revealed that the majority of altered proteins were linked to many cascade regulatory pathways including the mitochondrial energy metabolism and redox regulation by the EGFr/PI3K/AKT/SREBP-1 signaling pathway; protein folding by the heat shock response/ubiquitin/proteasome pathway; cytoskeleton structure, transcriptional regulation, and neuronal development by the MAPK/ERK signaling pathway; excitotoxicity; signal transduction by both WnT and GnRH signaling pathways; and hematopoiesis regulation and inflammatory mediation by chemokine and cytokine signaling pathways.

IDH mutations were considered important early events in glioma tumor initiation, and hence much efforts have been made to better understand their molecular mechanism and explore potential therapeutic avenues, namely, targeting the HIF-1α pathway,[9,130] or the altered metabolic sites via inhibition of the antioxidant activity, or the NAD^+ salvage pathway,[8,9] or the use of demethylating agents.[9] Drugs inhibiting Keap1-Nrf2 protein−protein interaction[129] and mutated IDH1/2 enzymes have entered clinical trials as novel classes for glioma therapy.[8,9] Our findings highlight other valuable therapeutic approaches such as perturbing ER homeostasis by purine analogues, regulating the KEAP1/Nrf2/ARE pathway, or using drug combinations that exert synergistic effects on more than one target simultaneously such as drug inhibitors of the PI3K/AKT/mTOR pathway, altering the chaperoning function, calmodulin and neuroserpin effects, or drugs mimicking the cystatin activity. Interestingly, targeting the apoptogenic pathways, in particular, MAPK and EGFR in the GnRH signaling pathway, may be an effective tool. Immunotherapy target could also be envisaged toward the identified hub proteins/genes to gain two advantages: first, a preventive therapy against recurrence of these diffuse infiltrating tumors, and second, to avoid damage to normal NSCs and progenitor cells. All of these predicted strategies may warrant further investigations and provide a great opportunity for revolutionary approaches to counteract the growth of IDH mutant high-grade gliomas.

Overall, the study may better define the role of IDH mutations in gliomagenesis and pave the way for effective new anticancer agents and diagnostic approaches to improve standard treatment and overall survival.

APPENDICES

$$V\ (\mu m^2) = \frac{4}{3} \times \pi\ r^3 \tag{A}$$

$$\text{CV in \%} = \frac{\text{standard deviation of spheroid diameter}}{\text{mean spheroid diameter}} \times 100$$

V: volume

r: radius

CV: coefficient of variation

(B)

ASSOCIATED CONTENT

Data Availability Statement

The data that support the findings of this study are openly available.

Supporting Information

The Supporting Information is available free of charge at https://pubs.acs.org/doi/10.1021/acs.jproteome.3c00395.

Experimental methods of neurospheroid culture protocols; Table 1: Selected patients' characteristics; Table 2 List of 24 identified proteins at upregulation; Table 3: List of 37 identified proteins expressed only in the treated neurospheroids; Table 4: Description of some of the identified proteins' functions; Figure S1: Additional figure of Venn diagrams; Figure S2: Additional figure of gene ontology (GO) term enrichement analysis; Figure S3: Additional figure of inter-relational pathway enrichment analysis; and references (PDF)

Accession Codes

Data that support the finding of this study, including peptide sequencing and protein identification, are openly available at the ProteomeXchange Consortium via the MassIVE partner repository (for shotgun proteomics data) at: https://massive.ucsd.edu/ProteoSAFe/QueryPXD?id=PXD038878. With the data set identifier: **Username: MSV000090924**_reviewer, **Password:** REVIEWER789.

AUTHOR INFORMATION

Corresponding Author

Kaouthar Louati − *Laboratory of Pharmacology, Analytics and Galenic Drug Development- LR12ES09, Faculty of Pharmacy, University of Monastir, 5000 Monastir, Tunisia;* orcid.org/0000-0001-5085-4766; Phone: +21692761162; Email: kaoutharlouati66@gmail.com, kaouthar.louati@fphm.u-monastir.tn

Authors

Amina Maalej − *Laboratory of Environmental Bioprocesses, Centre of Biotechnology of Sfax, 3018 Sfax, Tunisia*

Fatma Kolsi − *Department of Neurosurgery, Habib Bourguiba University Hospital, 3089 Sfax, Tunisia; Faculty of Medicine, University of Sfax, 3029 Sfax, Tunisia*

https://doi.org/10.1021/acs.jproteome.3c00395
J. Proteome Res. 2023, 22, 3534−3558

Rim Kallel − *Laboratory of Pathological Anatomy and Cytology, Habib Bourguiba University Hospital, 3089 Sfax, Tunisia; Faculty of Medicine, University of Sfax, 3029 Sfax, Tunisia*
Yassine Gdoura − *Department of Neurosurgery, Habib Bourguiba University Hospital, 3089 Sfax, Tunisia; Faculty of Medicine, University of Sfax, 3029 Sfax, Tunisia*
Mahdi Borni − *Department of Neurosurgery, Habib Bourguiba University Hospital, 3089 Sfax, Tunisia; Faculty of Medicine, University of Sfax, 3029 Sfax, Tunisia*
Leila Sellami Hakim − *Laboratory of Pathological Anatomy and Cytology, Habib Bourguiba University Hospital, 3089 Sfax, Tunisia*
Rania Zribi − *Higher Institute of Applied Studies to Humanities of Tunis (ISEAHT), University of Tunis, 1005 Tunis, Tunisia*
Sirine Choura − *Laboratory of Environmental Bioprocesses, Centre of Biotechnology of Sfax, 3018 Sfax, Tunisia*
Sami Sayadi − *Biotechnology Program, Center for Sustainable Development, College of Arts and Sciences, Qatar University, 2713 Doha, Qatar*
Mohamed Chamkha − *Laboratory of Environmental Bioprocesses, Centre of Biotechnology of Sfax, 3018 Sfax, Tunisia*
Basma Mnif − *Department of Bacteriology, Habib Bourguiba University Hospital, 3089 Sfax, Tunisia; Faculty of Medicine, University of Sfax, 3029 Sfax, Tunisia*
Zouheir Khemakhem − *Legal Medicine Department, Habib Bourguiba University Hospital, 3089 Sfax, Tunisia; Faculty of Medicine, University of Sfax, 3029 Sfax, Tunisia*
Tahya Sellami Boudawara − *Laboratory of Pathological Anatomy and Cytology, Habib Bourguiba University Hospital, 3089 Sfax, Tunisia; Faculty of Medicine, University of Sfax, 3029 Sfax, Tunisia*
Mohamed Zaher Boudawara − *Department of Neurosurgery, Habib Bourguiba University Hospital, 3089 Sfax, Tunisia; Faculty of Medicine, University of Sfax, 3029 Sfax, Tunisia*
Fathi Safta − *Laboratory of Pharmacology, Analytics and Galenic Drug Development- LR12ES09, Faculty of Pharmacy, University of Monastir, 5000 Monastir, Tunisia*

Complete contact information is available at: https://pubs.acs.org/10.1021/acs.jproteome.3c00395

Author Contributions

K.L. (the corresponding author): conceptualization, investigation, writing original draft, methodology, formal analysis, data curation, writing—review and editing. F.K., Y.G., M.B., and B.M.: investigation, resources. R.K., L.S.H., and T.S.B.: validation. A.M. and S.C.: formal analysis, software. R.Z.: writing—review and editing. S.S.: resources. M.C.: resources, project administration. M.Z.B.: supervision. Z.K.: project administration, visualization. F.S.: supervision. All authors have approved the final article.

Funding

This research did not receive any specific grant from funding agencies in public, commercial, or not-for-profit sectors.

Notes

The authors declare no competing financial interest.

■ ACKNOWLEDGMENTS

The study was supported by the Tunisian Ministry of Higher Education and the Ministry of Health. Our deepest and most sincere gratitude go to (1) our respresentative authorties of the medical ethics committee: Dr Khalil Nouri and Dr Zouhir Bahloul; (2) the head of the Pathological Anatomy Department and Cytology Laboratory in Habib Bourguiba medium hospital and her team due to their support in the histological diagnosis; (3) neurosurgeons: all of our neurosurgical doctors who have performed successful surgeries by taking into consideration their patients' safety, and the entire team in the neurosurgery department for their help; (4) Mrs. S. C., Mrs. A.M., and Mr. M.C. for their technical assistance and help in providing the necessary materials for cell culture in the biotechnology center, Sfax, Tunisia; (5) Mrs. R.Z. for proof-reading this article; (6) the pharmaceutical team of Habib Bourguiba University hospital for their help in providing the necessary surgical materials. (7) I am also immensely grateful to Dr Lively J and Ren S. for performing the facility analysis (Proteomics, USA). My special thanks to Mrs Coveny C. and Dr Boocock D. at the University of Nottingham, U.K., for supporting my knowledge in cancer research and proteomics-based MS analysis.

■ ABBREVIATIONS

3D	three-dimensional
ACN	acetonitrile
ACO	aconitase
AKT	serine/threonine kinase 1
ALDH	aldehyde dehydrogenase
ALDOC	aldolase, fructose-bisphosphate C
AMPAR	A-amino-3-hydroxy-5-methyl-4-isoxazole-propionic acid receptor
ANXA	annexin
AOC	amine oxidase
AP2	adaptor-related protein complexes
ARL6IP5	ADP ribosylation factor like gtpase-6 interacting protein 5
ARE-Nrf2-NF-Kb	antioxidant-responsive element/nuclear factor-erythroid-2-related factor 2/nuclear factor-kappa light chain enhancer of activated B cells
ASK1	apoptosis signal-regulating kinase 1
BP	biological process
CAND1	cullin-associated and neddylation-dissociated 1
CAPNS	calpains
CBR1	carbonyl reductase 1
CC	cellular compnent
C/EBP	CCAAT-enhancer-bindng protein
CFHR1	complement factor H-related 1
CKB	creatine kinase B
CRYL1	crystallin lambda 1
CV	coefficient of variation
CYB5B	cytochrome B5 type B
DLM	deltamethrin
DMEM	Dulbecco's modified eagle's medium-high glucose
DTT	DL-dithiothreitol
EGF	epidermal growth factor
EGFR	epidermal growth factor receptor
ERAD	endoplasmic reticulum-associated degradation
ENO	enolase
ERK	extracellular-signal-regulated kinase
ERLIN	ER lipid raft associated
EZR	ezrin

https://doi.org/10.1021/acs.jproteome.3c00395
J. Proteome Res. 2023, 22, 3534−3558

FA	formic acid
FAK	focal adhesion kinase
FBS	fetal bovine serum
FC	fold change
FDR	false discovery rate
FGF	fibroblast growth factor
GAPDH	glyceraldehyde-3-phosphate dehydrogenase
GDP2	GDP dissociation inhibitor 2
GBM	glioblastoma
GNAQ	G protein subunit alpha Q
GnRH	gonadotropin-releasing hormone
GO	gene ontology
GRHPR	glyoxylate and hydroxypyruvate reductase
GSCs	glioblastoma stem-like cells
GSH	glutathione
GSS	glutathione synthetase
GSTM2	glutathione S-transferase Mu 2
H&E	hematoxylin and eosin
HADHB	hydroxyacyl-CoA dehydrogenase subunit β
HCD	energy collision-induced dissociation
HIST	histamine
HLA-DRA	major histocompatibility complex, class II, DR α
HMGCR	3-hydroxy-3-methylglutaryl-CoA reductase
2HG	D-(R)-2-hydroxyglutarate
Hsps	heat shock proteins
ICAM1	intercellular adhesion molecule 1
IMD	imidacloprid
IAA	iodoacetamide
IDH1	isocitrate dehydrogenase 1
IHC	immunohistochemical
IMD	imidacloprid
IL	interleukin
IRE1	inositol-requiring enzyme type 1
JAK-STAT	janus kinase-signal transducer and activator of transcription
JNK	C-Jun NH(2)-terminal kinase
KEAP1	kelch-like ECH-associating protein-1
KNG1	kininogen 1
LDH	lactate dehydrogenase
LMNA	lamin
LTF	lactotransferrin isoform 2
MAOB	monoamine oxidase B
MAPK	mitogen-activated protein kinase
MDH2	malate dehydrogenase 2
MF	molecular function
MMP	matrix metallopeptidase
MNG	meningioma
MS	mass spectrometry
mTOR	mechanistic target of rapamycin kinase
$NADP^+$	nicotinamide adenine dinucleotide phosphate
NAP1L4	nucleosome assembly protein-1 like 4
NEAA	nonessential amino acid
NMDAR	*N*-Methyl-D-Aspartate Receptor
NPLOC4	NPL4 homolog, ubiquitin recognition factor
NO	nitric oxide
NNOS	neural nitric oxide synthase
OP	organophosphorus
OCT4	ctamer-binding transcription factor 4
PCYOX1	prenylcysteine oxidase 1
PDGFR	platelet-derived growth factor receptor β
PEA-15	proliferation and apoptosis adaptor protein 15
PPAR	peroxisome proliferator-activated receptor
PGK1	phosphoglycerate kinase
PGAM5	phosphoglycerate mutase 5
PBS	phosphate-buffered saline
PLC	phospholipase C
PHPT1	phosphohistidine phosphatase 1
PI3K	phosphoinositide-3-kinase
PKA	protein kinase A
PSMF1	proteasome inhibitor subunit 1
PSMD5	proteasome 26s subunit, non-atpase 5
PKC	protein kinase C
PPI	protein−protein interaction
PTM	post-transitional modification
PYGB	glycogen phosphorylase B
RAB1A	member RAS oncogene family
RDX	radixin
ROS	reactive oxygen species
RTK	receptor-tyrosine kinase
RNS	reactive nitrogen species
RRAS	ras-related
RTN4	reticulon 4
SEL1L	adaptor subunit OfERAD E3 ubiquitin ligase
STAT1	signal transducers and activators of transcription 1
SOD	superoxide dismutase
SOX2	SRY-box transcription factor 2
SLC	solute carrier
SPARC	secreted protein acidic and cysteine-rich
SPTAN1	spectrin Alpha, nonerythrocytic 1
SREBP	sterol regulatory element-binding transcription factor
SD	standard deviation
STIP1	stress-induced phosphoprotein 1
STRING	search tool for the retrieval of interacting genes
STAT3	signal transducer and activator of transcription 3
TGFB	transforming growth factor β 1
tPA	tissue plasminogen activator
TMEM43	transmembrane protein 43
TMZ	temozolomide
TNFα	tumor necrosis factor alpha
TNFRSF	TNF receptor superfamily
UHPLC-MS/MS	ultrahigh-performance liquid chromatography coupled to tandem mass spectrometry
VEGFA	vascular endothelial growth factor A
VEGFR	vascular endothelial growth factor R
VIM	vimentin
λ-CYH	lambda-cyhalothrin

REFERENCES

(1) Joo, K. M.; Kim, J.; Jin, J.; et al. Patient-specific orthotopic glioblastoma xenograft models recapitulate the histopathology and biology of human glioblastomas in situ. *Cell Rep.* **2013**, *3* (1), 260−273.
(2) Niclou, S. P.; Fack, F.; Rajcevic, U. Glioma proteomics: Status and perspectives. *J. Proteomics* **2010**, *73*, 1823−1838.
(3) Bhatia, P.; Bernier, M.; Sanghvi, M.; et al. Breast cancer resistance protein (BCRP/ABCG2) localises to the nucleus in glioblastoma multiforme cells. *Xenobiotica.* **2012**, *42*, 748−755.

https://doi.org/10.1021/acs.jproteome.3c00395
J. Proteome Res. 2023, 22, 3534−3558

(4) Friedman, H. S.; Kerby, T.; Calvert, H. Temozolomide and treatment of malignant glioma. *Clin. Canc. Res.* **2000**, *6*, 2585−2597.
(5) Uribe, D.; Torres, A.; Rocha, J. D.; et al. Multidrug resistance in glioblastoma stem-like cells: role of the hypoxic microenvironment and adenosine signaling. *Mol. Aspects Med.* **2017**, *55*, 140−151.
(6) Stupp, R.; Hegi, M. E.; Gilbert, M. R.; Chakravarti, A. Chemoradiotherapy in malignant glioma: standard of care and future directions. *J. Clin Oncol.* **2007**, *25* (26), 4127−4136.
(7) Louis, D. N.; Perry, A.; Wesseling, P.; et al. The 2021 WHO Classification of Tumors of the Central Nervous System: a summary. *Neuro Oncol.* **2021**, *23* (8), 1231−1251.
(8) Han, S.; Liu, Y.; Cai, S. J.; et al. IDH mutation in glioma: molecular mechanisms and potential therapeutic targets. *Br. J. Cancer* **2020**, *122*, 1580−1589.
(9) Han, C. H.; Batchelor, T. T. Isocitrate dehydrogenase mutation as a therapeutic target in gliomas. *Chin. Clin. Oncol.* **2017**, *6* (3), 33.
(10) Li, Q.; Aishwarya, S.; Li, J. P.; et al. Gene Expression Profiling of Glioblastoma to Recognize Potential Biomarker Candidates. *Front Genet.* **2022**, *13*, No. 832742.
(11) Alphandéry, E. Glioblastoma treatments: an account of recent industrial developments. *Front. Pharmacol.* **2018**, *9*, 879.
(12) Pfeffer, C. M.; Singh, A. T. K. Apoptosis: A Target for Anticancer Therapy. *Int. J. Mol. Sci.* **2018**, *19* (2), 448.
(13) Madian, A. G.; Regnier, F. E. Proteomic identification of carbonylated proteins and their oxidation sites. *J. Proteome Res.* **2010**, *9* (8), 3766−3780.
(14) Tebourbi, O.; Sakly, M.; Rhouma, K. B. *Pesticides in the Modern World-Pests Control and Pesticides Exposure and Toxicity Assessment*, IntechOpen: London (UK), 2011. Molecular Mechanisms of Pesticide Toxicity, https://www.intechopen.com/books/430.
(15) Lee, H. S.; Namkoong, K.; Kim, D. H.; et al. Hydrogen peroxide-induced alterations of tight junction proteins in bovine brain microvascular endothelial cells. *Microvasc. Res.* **2004**, *68* (3), 231−238.
(16) Hashimoto, K.; Oshima, T.; Tomita, T.; et al. Oxidative stress induces gastric epithelial permeability through claudin-3. *Biochem. Biophys. Res. Commun.* **2008**, *376* (1), 154−157.
(17) Doğanlar, Z. B.; Doğanlar, O.; Tozkir, H.; et al. Nonoccupational Exposure of Agricultural Area Residents to Pesticides: Pesticide Accumulation and Evaluation of Genotoxicity. *Arch. Environ. Contam. Toxicol.* **2018**, *75* (4), 530−544.
(18) Abdel-Halim, K. Y.; Osman, S. R. Cytotoxicity and Oxidative Stress Responses of Imidacloprid and Glyphosate in Human Prostate Epithelial WPM-Y.1 Cell Line. *J. Toxicol.* **2020**, *2020*, No. 4364650.
(19) Subbarao Sreedhar, A.; Sreedhar, A. S.; Kalmár, E.; Csermely, P. Hsp90 isoforms: functions, expression and clinical importance. *FEBS Lett.* **2004**, *562* (1−3), 11−15.
(20) García-García, C. R.; Parrón, T.; Requena, M.; et al. Occupational pesticide exposure and adverse health effects at the clinical, hematological and biochemical level. *Life Sci.* **2016**, *145*, 274−283.
(21) Katsuda, Y. Progress and future of pyrethroids. *Top Curr. Chem.* **2012**, *314*, 1−30.
(22) Verebová, V.; Staničová, J. The Effect of Neonicotinoid Insecticides on the Structure and Stability of Bio-Macromolecules. *Insecticides - Impact and Benefits of Its Use for Humanity*, Ranz, R. E. R., Ed.; IntechOpen: London, 2021; Available from: https://www.intechopen.com/chapters/78683.
(23) He, F. Synthetic pyrethroids. *Toxicology* **1994***91*43.
(24) Wang, Y.; Chen, C.; Qian, Y.; et al. Toxicity of mixtures of λcyhalothrin, imidacloprid and cadmium on the earthworm Eisenia fetida by combination index (CI)-isobologram method. *Ecotoxicol. Environ. Safe.* **2015**, *111*, 242−247.
(25) Igbedioh, S. O. Effects of agricultural pesticides on humans, animals, and higher plants in developing countries. *Arch. Environ. Health* **1991**, *46* (4), 218−224.
(26) World Health Organization & United Nations Environment Programme. *Public Health Impact of Pesticides Used in Agriculture*. World Health Organization [internet], Geneva; 1990; p. 88. Available from: https://apps.who.int/iris/handle/10665/39772.
(27) ATSDR (Agency for Toxic Substances and Disease Registry). *Toxicological Profile for Pyrethrins and Pyrethroids*. Department of Health and Human Services [Internet]. Atlanta: Gerogia, [cited 2003 September]. Available from: https://www.atsdr.cdc.gov/toxprofiles/tp155.pdf.
(28) Stivaktakis, P. D.; Kavvalakis, M. P.; Tzatzarakis, M. N.; et al. Long-term exposure of rabbits to imidaclorpid as quantified in blood induces genotoxic effect. *Chemosphere.* **2016**, *149*, 108−113.
(29) Aouey, B.; Fares, E.; Chtourou, Y.; et al. Lambda-cyhalothrin exposure alters purine nucleotide hydrolysis and nucleotidase gene expression pattern in platelets and liver of rats. *Chem. Biol. Interact.* **2019**, *311*, No. 108796.
(30) Özdemir, S.; Altun, S.; Arslan, H. Imidacloprid exposure cause the histopathological changes, activation of TNF-α, iNOS, 8-OHdG biomarkers, and alteration of caspase 3, iNOS, CYP1A, MT1 gene expression levels in common carp (Cyprinus carpio L.). *Toxicol. Rep.* **2018**, *5*, 125−133.
(31) Zheng, M.; Qin, Q.; Zhou, W.; et al. Metabolic disturbance in hippocampus and liver of mice: A primary response to imidacloprid exposure. *Sci. Rep.* **2020**, *10*, No. 5713.
(32) Godovac-Zimmermann, J.; Brown, L. R. Perspectives for mass spectrometry and functional proteomics. *Mass Spectrom Rev.* **2001**, *20* (1), 1−57.
(33) Roper, S. J.; Coyle, B. Establishing an in vitro 3D spheroid model to study medulloblastoma drug response and tumor dissemination. *Current Protocols* **2022**, *2*, No. e357.
(34) The Human Protein Atlas (version 21.1). Available from: https://www.proteinatlas.org/.
(35) PANTHER Database (Version 17.0). http://www.pantherdb.org.
(36) Zhou, Y.; Zhou, B.; Pache, L.; et al. Metascape provides a biologist-oriented resource for the analysis of systems-level datasets. *Nat. Commun.* **2019**, *10* (1), No. 1523.
(37) METASCAPE. A Gene Annotation & Analysis Resource. Available from: https://metascape.org/gp/index.html#/main/step1.
(38) Bindea, G.; Mlecnik, B.; Hackl, H.; et al. ClueGO: a Cytoscape plug-in to decipher functionally grouped geneontology and pathway annotation networks. *Bioinformatics* **2009**, *25* (8), 1091−1093.
(39) Bindea, G.; Galon, J.; Mlecnik, B. CluePedia Cytoscape plugin: pathwayinsights using integrated experimental and in silico data. *Bioinformatics* **2013**, *29* (5), 661−663.
(40) STRING database (Version 11.0). Available from https://string-db.org.
(41) Collins, A. T.; Berry, P. A.; Hyde, C.; et al. Prospective identification of tumorigenic prostate cancer stem cells. *Cancer Res.* **2005**, *65*, 10946−10951.
(42) Richardson, G. D.; Robson, C. N.; Lang, S. H.; et al. CD133, a novel marker for human prostatic epithelial stem cells. *J. Cell Sci.* **2004**, *117*, 3539−3545.
(43) Rizzo, S.; Attard, G.; Hudson, D. L. Prostate epithelial stem cells. *Cell Prolif.* **2005**, *38*, 363−374.
(44) O'Brien, C. A.; Pollett, A.; Gallinger, S.; Dick, J. E. A human colon cancer cell capable of initiating tumour growth in immunodeficient mice. *Nature* **2007**, *445*, 106−110.
(45) Ghosh, N.; Matsui, W. Cancer stem cells in multiple myeloma. *Cancer Lett.* **2009**, *277* (1), 1−7.
(46) Schatton, T.; Murphy, G. F.; Frank, N. Y.; et al. Identification of cells initiating human melanomas. *Nature* **2008**, *451*, 345−349.
(47) Bertolini, G.; Roz, L.; Perego, P.; et al. Highly tumorigenic lung cancer CD133+ Cells display stem-like features and are spared by cisplatin treatment. *Proc. Natl. Acad. Sci. U.S.A.* **2009**, *106*, 16281−16286.
(48) Friedrich, J.; Seidel, C.; Ebner, R.; Kunz-Schughart, L. A. Spheroid-based drug screen: considerations and practical approach. *Nat. Protoc.* **2009**, *4* (3), 309−324.
(49) Zanoni, M.; Piccinini, F.; Arienti, C.; et al. 3D tumor spheroid models for in vitro therapeutic screening: a systematic approach to enhance the biological relevance of data obtained. *Sci. Rep.* **2016**, *6*, No. 19103.

https://doi.org/10.1021/acs.jproteome.3c00395
J. Proteome Res. 2023, 22, 3534−3558

(50) Vinci, M.; Box, C.; Zimmermann, M.; Eccles, S. A. Tumor spheroid-based migration assays for evaluation of therapeutic agents. *Methods Mol. Biol.* **2013**, *986*, 253.
(51) Pavon, L. F.; Marti, L. C.; Sibov, T. T.; et al. In vitro Analysis of Neurospheres Derived from Glioblastoma Primary Culture: A Novel Methodology Paradigm. *Front Neurol.* **2014**, *4*, 214.
(52) Tang, X.; Zuo, C.; Fang, P.; et al. Targeting Glioblastoma Stem Cells: A Review on Biomarkers, Signal Pathways and Targeted Therapy. *Front Oncol.* **2021**, *11*, No. 701291.
(53) Vinci, M.; Gowan, S.; Boxall, F.; et al. Advances in establishment and analysis of three-dimensional tumor spheroid-based functional assays for target validation and drug evaluation. *BMC Biol.* **2012**, *10*, 29−49.
(54) Luchman, H. A.; Stechishin, O. D.; Dang, N. H.; et al. An in vivo patient-derived model of endogenous IDH1-mutant glioma. *Neuro Oncol.* **2012**, *14* (2), 184−191.
(55) Jacob, F.; Salinas, R. D.; Zhang, D. Y.; et al. A Patient-Derived Glioblastoma Organoid Model and Biobank Recapitulates Inter- and Intra-tumoral Heterogeneity. *Cell* **2020**, *180* (1), 188−204.e22.
(56) Xiao, Z. Y.; Chen, X. J.; Pan, Q.; et al. Expression of Nestin, CD133 and Sox2 in Meningiomas. *Turk Neurosurg.* **2018**, *28* (6), 910−914.
(57) Ehteram, H.; Aslanbeigi, F.; Ghoochani Khorasani, E.; et al. Expression and Prognostic Significance of Stem Cell Marker CD133 in Survival Rate of Patients with Colon Cancer. *Oncol. Ther.* **2022**, *10*, 451−461.
(58) Neradil, J.; Veselska, R. Nestin as a marker of cancer stem cells. *Cancer Sci.* **2015**, *106* (7), 803−811.
(59) Favaro, R.; Appolloni, I.; Pellegatta, S.; et al. Sox2 is required to maintain cancer stem cells in a mouse model of high-grade oligodendroglioma. *Cancer Res.* **2014**, *74* (6), 1833−1844.
(60) Brehar, F. M.; Arsene, D.; Brinduse, L. A.; et al. Immunohistochemical analysis of GFAP-delta and nestin in cerebral astrocytomas. *Brain Tumor Pathol.* **2015**, *32* (2), 90−98.
(61) Mariani, M.; Karki, R.; Spennato, M.; et al. Class III beta-tubulin in normal and cancer tissues. *Gene* **2015**, *563* (2), 109−114.
(62) Cantor, J. R.; Sabatini, D. M. Cancer cell metabolism: one hallmark, many faces. *Cancer Discovery* **2012**, *2* (10), 881−898.
(63) Jang, M.; Kim, S. S.; Lee, J. Cancer cell metabolism: implications for therapeutic targets. *Exp Mol. Med.* **2013**, *45* (10), No. e45.
(64) Zhang, F.; Du, G. Dysregulated lipid metabolism in cancer. *World J. Biol. Chem.* **2012**, *3* (8), 167−174.
(65) Oishi, Y.; Spann, N. J.; Link, V. M.; et al. SREBP1 Contributes to Resolution of Pro-inflammatory TLR4 Signaling by Reprogramming Fatty Acid Metabolism. *Cell Metab.* **2017**, *25* (2), 412−427.
(66) Fu, Y.; Zou, T.; Shen, X.; et al. Lipid metabolism in cancer progression and therapeutic strategies. *MedComm.* **2021**, *2* (1), 27−59.
(67) Broadfield, L. A.; Pane, A. A.; Talebi, A.; et al. Lipid metabolism in cancer: New perspectives and emerging mechanisms. *Dev Cell.* **2021**, *56* (10), 1363−1393.
(68) Gaetani, P.; Butti, G.; Chiabrando, C.; et al. A study on the biological behavior of human brain tumors. Part I. Arachidonic acid metabolism and DNA content. *J. Neurooncol.* **1991**, *10* (3), 233−240.
(69) Polisetty, R. V.; Gautam, P.; Sharma, R.; et al. LC-MS/MS analysis of differentially expressed glioblastoma membrane proteome reveals altered calcium signaling and other protein groups of regulatory functions. *Mol. Cell Proteomics* **2012**, *11* (6), No. M111.013565.
(70) Chiurchiù, V.; Leuti, A.; Maccarrone, M. Bioactive Lipids and Chronic Inflammation: Managing the Fire Within. *Front Immunol.* **2018**, *9*, 38.
(71) Hisano, Y.; Hla, T. Bioactive lysolipids in cancer and angiogenesis. *Pharmacol Ther.* **2019**, *193*, 91−98.
(72) Baek, A. E.; Yu, Y. A.; He, S.; et al. The cholesterol metabolite 27 hydroxycholesterol facilitates breast cancer metastasis through its actions on immune cells. *Nat. Commun.* **2017**, *8* (1), No. 864.
(73) Khan, I.; Steeg, P. S. Endocytosis: a pivotal pathway for regulating metastasis. *Br. J. Cancer* **2021**, *124* (1), 66−75.
(74) Schapira, A. H. Mitochondrial disease. *Lancet* **2006**, *368* (9529), 70−82.
(75) Sperlágh, B. ATP-Mediated Signaling in the Nervous System. In *Handbook of Neurochemistry and Molecular Neurobiology*, Lajtha, A.; Vizi, E. S., Eds.; Springer: Boston, MA, 2008.
(76) Chedik, L.; Bruyere, A.; Le Vee, M.; et al. Inhibition of Human Drug Transporter Activities by the Pyrethroid Pesticides Allethrin and Tetramethrin. *PLoS One* **2017**, *12* (1), No. e0169480.
(77) Zhang, R.; Tremblay, T. L.; McDermid, A.; et al. Identification of differentially expressed proteins in human glioblastoma cell lines and tumors. *Glia* **2003**, *42* (2), 194−208.
(78) Walenta, S.; Wetterling, M.; Lehrke, M.; et al. High lactate levels predict likelihood of metastases, tumor recurrence, and restricted patient survival in human cervical cancers. *Cancer Res.* **2000**, *60* (4), 916−921.
(79) Brizel, D. M.; Schroeder, T.; Scher, R. L.; et al. Elevated tumor lactate concentrations predict for an increased risk of metastases in head-and-neck cancer. *Int. J. Radiat Oncol Biol. Phys.* **2001**, *51* (2), 349−353.
(80) Schwickert, G.; Walenta, S.; Sundfør, K.; et al. Correlation of high lactate levels in human cervical cancer with incidence of metastasis. *Cancer Res.* **1995**, *55* (21), 4757−4759.
(81) Nam, H. J.; Kim, Y. E.; Moon, B. S.; et al. Azathioprine antagonizes aberrantly elevated lipid metabolism and induces apoptosis in glioblastoma. *iScience* **2021**, *24* (3), No. 102238.
(82) Shimano, H.; Sato, R. SREBP-regulated lipid metabolism: convergent physiology - divergent pathophysiology. *Nat. Rev. Endocrinol.* **2017**, *13* (12), 710−730.
(83) Li, C.; Yang, W.; Zhang, J.; et al. SREBP-1 has a prognostic role and contributes to invasion and metastasis in human hepatocellular carcinoma. *Int. J. Mol. Sci.* **2014**, *15* (5), 7124−7138.
(84) Zhao, Q.; Lin, X.; Wang, G. Targeting SREBP-1-Mediated Lipogenesis as Potential Strategies for Cancer. *Front Oncol.* **2022**, *12*, No. 952371.
(85) Guo, D.; Bell, E. H.; Mischel, P.; Chakravarti, A. Targeting SREBP-1-driven lipid metabolism to treat cancer. *Curr. Pharm. Des.* **2014**, *20* (15), 2619−2626.
(86) Rahman, M.; Hasan, M. R. Cancer Metabolism and Drug Resistance. *Metabolites* **2015**, *5* (4), 571−600.
(87) Erickson, R. R.; Dunning, L. M.; Olson, D. A.; et al. In cerebrospinal fluid ER chaperones ERp57 and calreticulin bind beta-amyloid. *Biochem. Biophys. Res. Commun.* **2005**, *332* (1), 50−57.
(88) Park, C. J.; Seo, Y. S. Heat Shock Proteins: A Review of the Molecular Chaperones for Plant Immunity. *Plant Pathol. J.* **2015**, *31* (4), 323−333.
(89) Shen, L.; Chen, C.; Yang, A.; et al. Redox proteomics identification of specifically carbonylated proteins in the hippocampi of triple transgenic Alzheimer's disease mice at its earliest pathological stage. *J. Proteomics* **2015**, *123*, 101−113.
(90) Kim, E. K.; Choi, E. J. Pathological roles of MAPK signaling pathways in human diseases. *Biochim. Biophys. Acta* **2010**, *1802* (4), 396−405.
(91) Zhao, J.; Zhang, L.; Dong, X.; et al. High Expression of Vimentin is Associated With Progression and a Poor Outcome in Glioblastoma. *Appl. Immunohistochem Mol. Morphol.* **2018**, *26* (5), 337−344.
(92) Mazzucchelli, L. Protein S100A4: too long overlooked by pathologists? *Am. J. Pathol.* **2002**, *160* (1), 7−13.
(93) Benaud, C.; Gentil, B. J.; Assard, N.; et al. AHNAK interaction with the annexin 2/S100A10 complex regulates cell membrane cytoarchitecture. *J. Cell Biol.* **2004**, *164* (1), 133−144.
(94) Seker, F.; Cingoz, A.; Sur-Erdem, İ.; et al. Identification of SERPINE1 as a Regulator of Glioblastoma Cell Dispersal with Transcriptome Profiling. *Cancers* **2019**, *11* (11), 1651.
(95) Godinez, A.; Rajput, R.; Chitranshi, N.; et al. Neuroserpin, a crucial regulator for axogenesis, synaptic modelling and cell-cell interactions in the pathophysiology of neurological disease. *Cell. Mol. Life Sci.* **2022**, *79* (3), 172.
(96) Nicole, O.; Docagne, F.; Ali, C.; et al. The proteolytic activity of tissue-plasminogen activator enhances NMDA receptor-mediated signaling. *Nat. Med.* **2001**, *7* (1), 59−64.

https://doi.org/10.1021/acs.jproteome.3c00395
J. Proteome Res. 2023, 22, 3534−3558

(97) Chuang, H. W.; Hsia, K. T.; Liao, J. B.; et al. SERPINE2 Overexpression Is Associated with Poor Prognosis of Urothelial Carcinoma. *Diagnostics* **2021**, *11* (10), 1928.
(98) Mussunoor, S.; Murray, G. I. The role of annexins in tumour development and progression. *J. Pathol.* **2008**, *216* (2), 131−140.
(99) Díaz-Ramos, Á.; Roig-Borrellas, A.; et al. α-Enolase, a multifunctional protein: its role on pathophysiological situations. *J. Biomed Biotechnol.* **2012**, *2012*, No. 156795.
(100) Tanwar, M. K.; Gilbert, M. R.; Holland, E. C. Gene expression microarray analysis reveals YKL-40 to be a potential serum marker for malignant character in human glioma. *Cancer Res.* **2002**, *62* (15), 4364−4368.
(101) Bryant, J. A.; Finn, R. S.; Slamon, D. J.; et al. EGF activates intracellular and intercellular calcium signaling by distinct pathways in tumor cells. *Cancer Biol. Ther.* **2004**, *3* (12), 1243−1249.
(102) Ramos, R. N.; Rodriguez, C.; Hubert, M.; et al. CD163^{+} tumor-associated macrophage accumulation in breast cancer patients reflects both local differentiation signals and systemic skewing of monocytes. *Clin. Transl. Immunol.* **2020**, *9* (2), No. e1108.
(103) Rudzińska, M.; Parodi, A.; Soond, S. M.; et al. The Role of Cysteine Cathepsins in Cancer Progression and Drug Resistance. *Int. J. Mol. Sci.* **2019**, *20*, 3602.
(104) Flannery, T.; Gibson, D.; Mirakhur, M.; et al. The clinical significance of cathepsin S expression in human astrocytomas. *Am. J. Pathol.* **2003**, *163* (1), 175−182.
(105) Nowicki, M. O.; Hayes, J. L.; Chiocca, E. A.; Lawler, S. Proteomic Analysis Implicates Vimentin in Glioblastoma Cell Migration. *Cancers* **2019**, *11* (4), 466.
(106) Sun, S.; Wong, T. S.; Zhang, X. Q.; et al. Protein alterations associated with Temozolomide resistance in subclones of human glioblastoma cell lines. *J. Neurooncol.* **2012**, *107* (1), 89−100.
(107) Chen, W.; Xia, T.; Wang, D.; et al. Human astrocytes secrete IL-6 to promote glioma migration and invasion through upregulation of cytomembrane MMP14. *Oncotarget* **2016**, *7* (38), 62425−62438.
(108) Cabral-Pacheco, G. A.; Garza-Veloz, I.; Castruita-De la Rosa, C.; et al. The Roles of Matrix Metalloproteinases and Their Inhibitors in Human Diseases. *Int. J. Mol. Sci.* **2020**, *21* (24), 9739.
(109) Camby, I.; Lefranc, F.; Titeca, G.; et al. Differential expression of S100 calcium-binding proteins characterizes distinct clinical entities in both WHO grade II and III astrocytic tumours. *Neuropathol. Appl. Neurobiol.* **2000**, *26* (1), 76−90.
(110) Cui, M.; Huang, J.; Zhang, S.; et al. Immunoglobulin Expression in Cancer Cells and Its Critical Roles in Tumorigenesis. *Front Immunol.* **2021**, *12*, No. 613530.
(111) Tripathi, P. H.; Akhtar, J.; Arora, J.; et al. Quantitative proteomic analysis of GnRH agonist treated GBM cell line LN229 revealed regulatory proteins inhibiting cancer cell proliferation. *BMC Cancer* **2022**, *22* (1), 133.
(112) Xu, J.; Fang, J.; Cheng, Z.; et al. Overexpression of the Kininogen-1 inhibits proliferation and induces apoptosis of glioma cells. *J. Exp Clin Cancer Res.* **2018**, *37* (1), 180.
(113) Reiss, N.; Llevi, L. N.; Shacham, S.; et al. Mechanism of mitogen-activated protein kinase activation by gonadotropin-releasing hormone in the pituitary of alphaT3−1 cell line: differential roles of calcium and protein kinase C. *Endocrinology* **1997**, *138* (4), 1673−1682.
(114) Li, F.; Ma, H.; Liu, J. Pyrethroid Insecticide Cypermethrin Modulates Gonadotropin Synthesis via Calcium Homeostasis and ERK1/2 Signaling in Lβ*T2Mouse Pituitary Cells. *Toxicol. Sci.* **2018**, *162* (1), 43−52.
(115) Weber, D.; Davies, M. J.; Grune, T.; et al. Determination of protein carbonyls in plasma, cell extracts, tissue homogenates, isolated proteins: focus on sample preparation and derivatization conditions. *Redox Biol.* **2015**, *5*, 367−380.
(116) Koff, J. L.; Ramachandiran, S.; Bernal-Mizrachi, L. A time to kill: targeting apoptosis in cancer. *Int. J. Mol. Sci.* **2015**, *16* (2), 2942−2955.
(117) Gaur, U.; Aggarwal, B. B. Regulation of proliferation, survival and apoptosis by members of the TNF superfamily. *Biochem. Pharmacol.* **2003**, *66* (8), 1403−1408.
(118) Locksley, R. M.; Killeen, N.; Lenardo, M. J. The TNF and TNF receptor superfamilies: integrating mammalian biology. *Cell* **2001**, *104* (4), 487−501.
(119) Guicciardi, M. E.; Gores, G. J. Life and death by death receptors. *FASEB J.* **2009**, *23* (6), 1625−1637.
(120) Obacz, J.; Avril, T.; Le Reste, P. J.; et al. Endoplasmic reticulum proteostasis in glioblastoma-From molecular mechanisms to therapeutic perspectives. *Sci. Signal.* **2017**, *10* (470), No. eaal2323.
(121) Peñaranda Fajardo, N. M.; Meijer, C.; Kruyt, F. A. The endoplasmic reticulum stress/unfolded protein response in gliomagenesis, tumor progression and as a therapeutic target in glioblastoma. *Biochem. Pharmacol.* **2016**, *118*, 1−8.
(122) Mactier, S.; Henrich, S.; Che, Y.; et al. Comprehensive proteomic analysis of the effects of purine analogs on human Raji B-cell lymphoma. *J. Proteome Res.* **2011**, *10* (3), 1030−1042.
(123) Tian, R.; Abarientos, A.; Hong, J.; et al. Genome-wide CRISPRi/a screens in human neurons link lysosomal failure to ferroptosis. *Nat. Neurosci.* **2021**, *24* (7), 1020−1034.
(124) Gholkar, A. A.; Cheung, K.; Williams, K. J.; et al. Fatostatin Inhibits Cancer Cell Proliferation by Affecting Mitotic Microtubule Spindle Assembly and Cell Division. *J. Biol. Chem.* **2016**, *291* (33), 17001−17008.
(125) Li, X.; Wu, J. B.; Chung, L. W.; Huang, W. C. Anti-cancer efficacy of SREBP inhibitor, alone or in combination with docetaxel, in prostate cancer harboring p53 mutations. *Oncotarget* **2015**, *6* (38), 41018−41032.
(126) Kaminska, B.; Czapski, B.; Guzik, R.; et al. Consequences of IDH1/2 Mutations in Gliomas and an Assessment of Inhibitors Targeting Mutated IDH Proteins. *Molecules* **2019**, *24* (5), 968.
(127) Sule, R. O.; Condon, L.; Gomes, A. V. A Common Feature of Pesticides: Oxidative Stress-The Role of Oxidative Stress in Pesticide-Induced Toxicity. *Oxid Med. Cell Longev.* **2022**, *2022*, No. 5563759.
(128) Liu, L.; Cao, Y.; Chen, C.; et al. Sorafenib blocks the RAF/MEK/ERK pathway, inhibits tumor angiogenesis, and induces tumor cell apoptosis in hepatocellular carcinoma model PLC/PRF/5. *Cancer Res.* **2006**, *66* (24), 11851−11858.
(129) Lu, M. C.; Ji, J. A.; Jiang, Z. Y.; You, Q. D. The Keap1-Nrf2-ARE Pathway as a Potential Preventive and Therapeutic Target: An Update. *Med. Res. Rev.* **2016**, *36* (5), 924−963.
(130) Awuah, W. A.; Toufik, A. R.; Yarlagadda, R.; Mikhailova, T.; Mehta, A.; Huang, H.; Kundu, M.; Lopes, L.; Benson, S.; Mykola, L.; Vladyslav, S.; Alexiou, A.; Alghamdi, B. S.; Hashem, A. M.; Md Ashraf, G. Exploring the role of Nrf2 signaling in glioblastoma multiforme. *Discov. Oncol.* **2022**, *13* (1), 94.
(131) Yu, C.; Xiao, J. H. The Keap1-Nrf2 System: A Mediator between Oxidative Stress and Aging. *Oxid Med. Cell Longev.* **2021**, *2021*, No. 6635460.
(132) Stępkowski, T. M.; Kruszewski, M. K. Molecular cross-talk between the NRF2/KEAP1 signaling pathway, autophagy, and apoptosis. *Free Radic. Biol. Med.* **2011**, *50* (9), 1186−1195.
(133) Song, M. Y.; Lee, D. Y.; Chun, K. S.; Kim, E. H. The Role of NRF2/KEAP1 Signaling Pathway in Cancer Metabolism. *Int. J. Mol. Sci.* **2021**, *22*, 4376.
(134) Sule, R. O.; Condon, L.; Gomes, A. V. A Common Feature of Pesticides: Oxidative Stress-The Role of Oxidative Stress in Pesticide-Induced Toxicity. *Oxid Med. Cell Longev.* **2022**, *2022*, No. 5563759.
(135) Chi, C. C.; Chou, C. T.; Liang, W. Z.; Jan, C. R. Effect of the pesticide, deltamethrin, on Ca2+ signaling and apoptosis in OC2 human oral cancer cells. *Drug Chem. Toxicol.* **2014**, *37* (1), 25−31.
(136) Hsu, S. S.; Chou, C. T. Deltamethrin-Induced [C^{2+}]i Rise and Death in HGB Human Glioblastoma Cells. *Chin J. Physiol.* **2012**, *55* (4), 294−304.
(137) Wang, J.; Xu, X.; Jia, W.; et al. Calcium-/Calmodulin-Dependent Protein Kinase II (CaMKII) Inhibition Induces Learning and Memory Impairment and Apoptosis. *Oxid. Med. Cell. Longevity* **2021**, *2021*, 1.
(138) Yokokura, S.; Yurimoto, S.; Matsuoka, A.; et al. Calmodulin antagonists induce cell cycle arrest and apoptosis in vitro and inhibit

https://doi.org/10.1021/acs.jproteome.3c00395
J. Proteome Res. 2023, 22, 3534−3558

tumor growth in vivo in human multiple myeloma. *BMC Cancer* **2014**, *14*, 882.
(139) Villalobo, A.; Berchtold, M. W. The Role of Calmodulin in Tumor Cell Migration, Invasiveness, and Metastasis. *Int. J. Mol. Sci.* **2020**, *21* (3), 765.
(140) He, Q.; Li, Z. The dysregulated expression and functional effect of CaMK2 in cancer. *Cancer Cell Int.* **2021**, *21*, 326.
(141) Annabi, B.; Pilorget, A.; Bousquet-Gagnon, N.; et al. Calmodulin inhibitors trigger the proteolytic processing of membrane type-1 matrix metalloproteinase, but not its shedding in glioblastoma cells. *Biochem. J.* **2001**, *359*, 325−333.
(142) Hamilton, G.; Colbert, J. D.; Schuettelkopf, A. W.; Watts, C. Cystatin F is a cathepsin C-directed protease inhibitor regulated by proteolysis. *EMBO J.* **2008**, *27* (3), 499−508.
(143) Nishio, C.; Yoshida, K.; Nishiyama, K.; et al. Involvement of cystatin C in oxidative stress-induced apoptosis of cultured rat CNS neurons. *Brain Res.* **2000**, *873* (2), 252−262.
(144) Talaei, S.; Mellatyar, H.; Asadi, A.; et al. Spotlight on 17-AAG as an Hsp90 inhibitor for molecular targeted cancer treatment. *Chem. Biol. Drug Des.* **2019**, *93* (5), 760−786.
(145) Vinci, M.; Gowan, S.; Boxall, F.; et al. Advances in establishment and analysis of three-dimensional tumor spheroid-based functional assays for target validation and drug evaluation. *BMC Biol.* **2012**, *10*, 29.
(146) Strik, H.; Deininger, M.; Streffer, J.; et al. BCL-2 family protein expression in initial and recurrent glioblastomas: modulation by radiochemotherapy. *J. Neurol. Neurosurg. Psychiatry* **1999**, *67* (6), 763−768.
(147) Stegh, A. H.; Kesari, S.; Mahoney, J. E.; et al. Bcl2L12-mediated inhibition of effector caspase-3 and caspase-7 via distinct mechanisms in glioblastoma. *Proc. Natl. Acad. Sci. U.S.A.* **2008**, *105* (31), 10703−10708.
(148) Yang, Y.; Zong, M.; Xu, W.; et al. Natural pyrethrins induces apoptosis in human hepatocyte cells via Bax- and Bcl-2-mediated mitochondrial pathway. *Chem. Biol. Interact.* **2017**, *262*, 38−45.

https://doi.org/10.1021/acs.jproteome.3c00395
J. Proteome Res. 2023, 22, 3534−3558